

# TRANSPORT OF MAGNETIC FIELDS IN CONVECTIVE, ACCRETING SUPERNOVA CORES

Christopher Thompson

Physics and Astronomy, University of North Carolina CB3255, Chapel Hill, NC 27599;  
Canadian Institute for Theoretical Astrophysics, Toronto, ON M5S 3H8

Norman Murray

Canadian Institute for Theoretical Astrophysics, Toronto, ON M5S 3H8

## ABSTRACT

We consider the amplification and transport of a magnetic field in the collapsed core of a massive star, including both the region between the neutrinosphere and the shock, and the central, opaque core. An analytical argument explains why rapid convective overturns persist within a newly formed neutron star for roughly 10 seconds ( $> 10^3$  overturns), consistent with recent numerical models. A dynamical balance between turbulent and magnetic stresses within this convective layer corresponds to flux densities in excess of  $10^{15}$  G. Material accreting onto the core is heated by neutrinos and also becomes strongly convective. We compare the expected magnetic stresses in this convective ‘gain layer’ with those deep inside the neutron core.

Buoyant motions of magnetized fluid are greatly aided by the intense neutrino flux. We calculate the transport rate through a medium containing free neutrons, protons, and electrons, in the limiting cases of degenerate or non-degenerate nucleons. Fields stronger than  $\sim 10^{13}$  G are able to rise through the outer degenerate layers of the neutron core during the last stages of Kelvin-Helmholtz cooling (up to 10 seconds post-collapse), even though these layers have become stable to convection. We also find the equilibrium shape of a thin magnetic flux rope in the dense hydrostatic atmosphere of the neutron star, along with the critical separation of the footpoints above which the rope undergoes unlimited expansion against gravity. The implications of these results for pulsar magnetism are summarized, and applied to the case of late fallback over the first  $10^3 - 10^4$  s of the life of a neutron star.

*Subject headings:* supernova; dynamo; neutron star; stars-magnetically active

*Astrophysical Journal, in press*

## 1. Introduction

Young neutron stars are believed to be strongly magnetized, based on measurements of their spin behavior (Kulkarni 1992, and references therein) and the polarization of their pulsed emissions (Lyne & Manchester 1989). The inferred dipole fields are in the range  $10^{11} - 10^{14}$ G. In a broader sense, neutron star magnetic fields of this magnitude are weak. Consider, for example, a newly formed neutron star within which neutrinos of all types are temporarily trapped: near the neutrino photosphere (neutrinosphere) this dipole field makes only a tiny contribution to the hydrostatic stresses,  $B_{\text{dipole}}^2/8\pi P \sim 10^{-9}(B_{\text{dipole}}/10^{12} \text{ G})^2$ , as compared with  $\sim 10^{-6}$  in the Sun. Over the last several years there has been a growing accumulation of evidence pointing to the existence of neutron stars in which the magnetic fields are so strong as to be transported rapidly throughout the core and deep crust of the star, even at the remarkably short age of  $\sim 10^4$  yr. This evidence has come in several forms: the short but dramatically bright outbursts of the Soft Gamma Repeaters; the persistent, pulsed output of X-rays from these sources and the non-bursting Anomalous X-ray pulsars; and the rapid braking of the rotation of the SGRs and AXPs. These developments are exciting, in part, because direct physical measures of strong magnetic fields in isolated neutron stars such as radio pulsars have been difficult to obtain.

The physical origin of magnetism in neutron stars is difficult to pin down because there are few direct observational probes of the evolving cores of massive stars. Nonetheless, a simple physical argument points directly to the violent convective motions that develop in the supernova core as the predominant source of free energy. The kinetic energy carried by this convection (both inside the neutrinosphere of the nascent neutron star, and between the neutrinosphere and the shock) is  $\sim 100$  times greater relative to the gravitational binding energy than it is during any convective episode driven by nuclear burning (Thompson & Duncan 1993, hereafter TD93). From this perspective, the strength of the seed magnetic field (present, e.g., at the end of the main sequence evolution) becomes of secondary consequence to the final disposition of magnetic fields in the neutron star. There is growing empirical evidence – from chromospheric and coronal activity in fully convective stars (Delfosse et al. 1998; Küker & Rüdiger 1999) and from the small scale, intranetwork magnetic field of the Sun (e.g. Durney, de Young, & Roxburgh 1993) – that magnetic and turbulent stresses reach a dynamical balance in a fluid of very high magnetic Reynolds number, even if that fluid is slowly rotating.

In this paper, we consider afresh the transport of magnetic fields in the collapsed core of a supernova. We focus in particular on the role of the intense neutrino flux in facilitating transport of magnetic fields across convectively stable layers that would otherwise bury dynamo-generated magnetic fields. Before the supernova shock escapes to large radius, the

neutrinosphere is enveloped by a fairly thick layer of material ( $\Delta M \sim 0.01\text{-}0.1M_\odot$ ) which is stabilized to convection by a gradient in electron fraction  $Y_e$  (Keil, Janka & Mueller 1996, hereafter KJM). Even as the shock propagates outward, a reverse shock forms that can deposit up to  $\sim 0.1 M_\odot$  onto the neutron core over  $\sim 10^3$  s (Woosley & Weaver 1995; Fryer, Colgate, & Pinto 1999, and references therein).

The plan of this paper is as follows. Section 2 and the Appendix give a fresh analysis of persistent convection inside the neutrinosphere of a newly formed neutron star. We focus on the forcing of convection by secular neutrino cooling, when the lepton number gradient begins to stabilize the star but a negative entropy gradient persists. We connect our calculation to those of Lattimer & Mazurek (1981) and Reisenegger & Goldreich (1992), who calculate the Brunt-Väisälä frequency in hot and cold neutron stars. We also note that continuing fallback onto the neutron core will induce rapid convection outside the neutrinosphere that can deposit a strong (but tangled) magnetic field in the surface layers of the star.

The rate of radial transport of a magnetic field in and around the forming neutron core is calculated in detail in Section 3. Turbulent pumping moves magnetic flux outward rapidly through the convective core, in the direction of decreasing turbulent diffusivity (§3.1). Outside the neutrinosphere, neutrino absorption increases the entropy of a magnetic flux rope with respect to its surroundings and allows it to move outward through a stably stratified atmosphere (§3.2). At late times, when the optically thick interior of the star is no longer convective, neutrinos induce transformations between protons and neutrons that allow a strongly magnetized parcel of fluid to move across a stabilizing lepton number gradient (§3.3). The net result is that magnetic fields stronger than  $10^{13} - 10^{14}$  G will rise buoyantly to the surface of a newly formed neutron star. The equilibrium configuration of a magnetic flux rope that extends outward from the convective interior of the star through the dense outer atmosphere is addressed in Section 4.

We summarize in §5 the implications for pulsar magnetism, discussing the relative importance of the interior and exterior dynamos, and applying our results to the case of late fallback (over  $\sim 10^3 - 10^4$  s). The gravitational binding energy of the accreting material is converted to electron-type neutrinos, whose luminosity  $G\dot{M}M_{\text{NS}}/R_{\text{NS}} = 7 \times 10^{49} (\dot{M}/10^{-4} M_\odot\text{s}^{-1}) (M_{\text{NS}}/1.4 M_\odot) (R_{\text{NS}}/10 \text{ km})^{-1} \text{ erg s}^{-1}$  is smaller, by about two orders of magnitude, than the luminosity emitted during the prompt  $\sim 30$  s Kelvin-Helmholtz phase. Nonetheless, this neutrino flux is high enough to induce many convective overturns within  $\sim 100$  km of the neutron star (Thompson 2000, hereafter T00; §5), and thus to wind up a seed magnetic field within the accretion flow. As the result of the

## 2. Amplification of Magnetic Fields

The supernova core is subject to a violent convective instability inside the  $\nu$ -sphere, driven by optically thick neutrino cooling; and a distinct convective instability below the shock, triggered by heating by the outward-streaming neutrinos (Fig. 1). This second instability will persist as long as substantial accretion continues onto the neutron core, and the core remains a luminous source of neutrinos. We first show that entropy gradients will drive convection below the neutrinosphere of a young neutron star. We then consider the response of a magnetic field to instabilities either above or below the neutrinosphere.

### 2.1. Convection Inside the Neutrinosphere

The stability of a neutron star to convection depends on gradients in both entropy and composition. The key compositional parameter is the net lepton number per baryon,  $Y_\ell = Y_e + Y_{\nu_e}$ , where  $Y_e$  and  $Y_{\nu_e}$  are respectively the numbers of electrons and electron neutrinos per baryon. During the first  $\sim 10$  seconds, when the star is optically thick to neutrinos, it is unstable to convection (Wilson & Mayle 1988; Burrows 1987; TD93; KJM; Pons et al. 1999). The Ledoux criterion for convective instability is expressed most conveniently as

$$\frac{dS}{dR} + \frac{(\partial\rho/\partial Y_l)_{P,S}}{(\partial\rho/\partial S)_{P,Y_l}} \frac{dY_l}{dR} = \frac{dS}{dR} - \left( \frac{\partial S}{\partial Y_l} \right)_{P,\rho} \frac{dY_l}{dR} < 0. \quad (1)$$

(e.g. Lattimer & Mazurek 1981).

It is worth explaining here why this deep convective instability is generic, because its existence has been called into question on the basis of hydrodynamical simulations of the outer neutron core, at relatively low optical depth to neutrinos (Mezzacappa et al. 1998). Deep convection is distinct from the short-lived overturn which occurs where the weakening shock establishes a negative entropy gradient and which, according to some simulations such as those of Burrows, Hayes, & Fryxell (1995) and Bruenn & Mezzacappa (1994), may be quenched by neutrino diffusion in the first 20-50 ms after bounce. In deep convection, the gradients of  $Y_l$  and  $S$  both tend to be reduced (e.g. KJM), but are not entirely eliminated. Rather, they are constantly regenerated by radiative losses from the neutrinosphere. Thus, convection must continue until the magnitude of the radiative gradient drops below the adiabatic gradient. The reduction of the radiative gradient results primarily from the decrease in flux over the Kelvin time, which is of order ten seconds.

Ledoux convection is always encouraged by negative  $dS/dR$ , but the effect of  $dY_l/dR$  on convective instability depends on the temperature and composition. Negative  $dY_l/dR$

is quickly established in a cooling neutron core by neutrino transport at high  $Y_l$  and by chemical equilibrium between electrons, protons and neutrons at low  $Y_l \lesssim 0.1$  (where the lepton number is carried almost entirely by the electrons). The sign of the thermodynamic derivative  $(\partial S/\partial Y_\ell)_{P,\rho}$  is therefore crucial to the nature of the convective instability. The negative lepton-fraction gradient is de-stabilizing  $[(\partial S/\partial Y_\ell)_{P,\rho} < 0]$  if the neutrino chemical potential  $\mu_{\nu_e}$  is high enough *and* if the temperature is lower than a critical value  $T_\star$ . In this situation, where a compositional gradient is potentially the main driving force behind the convective instability, salt-finger effects may play an important role in its non-linear development (Wilson & Mayle 1988).

The critical temperature  $T_\star$  can be estimated analytically when the protons, neutrons, electrons, and electron neutrinos are all treated as ideal and almost degenerate fermi gases. As derived in Appendix A.2 (eq. [A35]), one has<sup>1</sup>

$$\begin{aligned} k_B T_\star &\simeq \frac{\mu_e}{\pi} \left[ 1 - \left( \frac{Y_e}{1 - Y_e} \right)^{2/3} \right]^{-1/2} \left[ \frac{3(2\mu_{\nu_e} - \mu_e)}{m_n c^2} \right]^{1/2} \\ &= 35 \left( \frac{n_b}{n_{\text{sat}}} \right)^{1/2} \left( \frac{2\mu_{\nu_e} - \mu_e}{\mu_e} \right)^{1/2} \text{ MeV} \quad (Y_e \simeq 0.1). \end{aligned} \quad (2)$$

Here  $\mu_e$  and  $\mu_{\nu_e}$  are the chemical potentials of the electrons and electron neutrinos, respectively. We have scaled the density to the nuclear saturation density  $n_{\text{sat}} = 1.6 \times 10^{38} \text{ cm}^{-3}$  (corresponding to a mass density  $m_n n_{\text{sat}} = 2.8 \times 10^{14} \text{ g cm}^{-3}$ ). This critical temperature is comparable to the initial peak temperature in the neutron core. Negative  $dY_l/dR$  induces convection below the temperature  $T_\star$ , but only as long as  $\mu_{\nu_e} > \frac{1}{2}\mu_e$ , or equivalently

$$Y_{\nu_e} > \frac{1}{16} Y_e. \quad (3)$$

In fact,  $Y_{\nu_e}$  falls below this bound quickly in the outer parts of the neutron core, in about 1 second according to the cooling models of Pons et al. (1999). Thereafter, the composition gradient becomes stabilizing (Lattimer & Mazurek 1981; Goldreich & Reisenegger 1992; KJM; see §A.4). However, we now show that a negative entropy gradient can drive convection in a multicomponent, noninteracting Fermi gas, even in the presence of a stabilizing composition gradient.

Such a “late phase” of convection occurs if the radiative temperature gradient is sufficiently super-adiabatic. The radiative gradient is set by the neutrino opacity, the energy

---

<sup>1</sup>Neglecting terms of the order of  $Y_{\nu_e}/Y_e$  and  $\mu_e/m_n c^2$ , but not  $\mu_{\nu_e}/\mu_e = (2Y_{\nu_e}/Y_e)^{1/3}$ .

flux, and the temperature:

$$F_{\text{rad}} = - \left( \frac{7N_\nu}{8} \right) \frac{16\sigma_{\text{SB}}T^4}{3} \left( \frac{1}{\langle n_b\sigma_\nu \rangle R} \right) \frac{d \ln T}{d \ln R}. \quad (4)$$

Here,  $\sigma_\nu$  is the neutrino cross section and the angular brackets indicate a Rosseland mean. During the intermediate stages of cooling, the energy flux is carried primarily by  $\mu$  and  $\tau$  neutrinos: their opacity is due to scattering and is smaller than the absorption opacity of  $\nu_e$  on neutrons above a temperature of  $\sim 10$  MeV (where the absorption is not Fermi-blocked by the degenerate electrons; Pons et al. 1999). In this situation, the effective number of neutrino species in expression (4) is  $N_\nu \simeq 2$ . However, the production rate of  $\mu$  and  $\tau$  neutrinos may be so low that they cannot carry the flux, in which case  $N_\nu = 1$ .

A negative entropy gradient is generated by steady radiative transport, as is easily seen from the following argument. The opacity of non-degenerate neutrinos scattering from degenerate nucleons scales as  $E_\nu^3$  (as compared with the  $E_\nu^2$  energy dependence of the weak neutral current in a non-degenerate plasma; Iwamoto 1981). The Rosseland mean free path is  $\langle \sigma \rangle(T) \simeq \sigma(E_\nu = 2k_B T)$  for a Fermi-Dirac distribution of neutrinos with temperature  $T$  and vanishing chemical potential. The mean-free path for neutron scattering is

$$\frac{1}{n_n \sigma(E_\nu)} = 2 \times 10^3 \left( \frac{E_\nu}{30 \text{ MeV}} \right)^{-3} \text{ cm} \quad (5)$$

at a density  $n_b = n_{\text{sat}}$  (we normalize to Fig. 12 of Reddy, Prakash, & Lattimer 1998). The radiative temperature gradient can, then, be directly related to the total radiative flux  $F_{\text{rad}} = L_\nu/4\pi R^2$ :

$$\left( \frac{d \ln T}{d \ln R} \right)_{\text{rad}} = -1.3 \left( \frac{N_\nu}{2} \right)^{-1} \left( \frac{L_\nu}{10^{52} \text{ erg s}^{-1}} \right) \left( \frac{T}{10 \text{ MeV}} \right)^{-1} \left( \frac{R}{10 \text{ km}} \right)^{-1}. \quad (6)$$

This radiative gradient must be compared with the gradient required to trigger convection in the face of a (possibly) stabilizing composition gradient. This convective temperature gradient is calculated by setting  $dS/dR = (\partial S/\partial Y_l)_{P,\rho} dY_l/dR$ . The entropy (per baryon) is provided mainly by free neutrons and protons, with respective abundances  $Y_n \simeq 1 - Y_e$  and  $Y_p = Y_e$ :

$$\frac{S}{k_B} \simeq \frac{\pi^2}{2} \left[ Y_e \left( \frac{k_B T}{\mu_p} \right) + (1 - Y_e) \left( \frac{k_B T}{\mu_n} \right) \right]. \quad (7)$$

Here, the  $\mu_p$ ,  $\mu_n$  are the chemical potentials of the degenerate protons and neutrons respectively. This critical temperature gradient for convection is calculated in Appendix A.3:

$$\left( \frac{d \ln T}{d \ln R} \right)_{\text{conv}} \simeq \frac{2}{3} \left( \frac{d \ln \rho}{d \ln R} \right) - \frac{Y_e^{1/3}}{Y_e^{1/3} + (1 - Y_e)^{1/3}} \times$$

$$\times \left[ 3Y_e \frac{\hbar^3 c n_b}{m_n (kT)^2} \left( \frac{\mu_e - 2\mu_{\nu_e}}{\mu_e} \right) + \frac{1}{3} \left\{ 1 - \left( \frac{Y_e}{1 - Y_e} \right)^{2/3} \right\} \right] \frac{d \ln Y_e}{d \ln R}, \quad (8)$$

Notice that the second term (proportional to  $d \ln Y_e / d \ln R$ ) is guaranteed to be stabilizing when  $d \ln Y_e / d \ln R < 0$  and  $2\mu_{\nu_e} < \mu_e$ . The coefficient

$$3Y_e \frac{\hbar^3 c n_b}{m_n (kT)^2} = 1.0 \left( \frac{n_b}{n_{\text{sat}}} \right) \left( \frac{Y_e}{0.1} \right) \left( \frac{k_B T}{20 \text{ MeV}} \right)^{-2}. \quad (9)$$

This analytical criterion indicates a slightly earlier end to convection than is found in the cooling models of Pons et al. (1999) (cf. their Figs. 9, 21, and 24). The value of  $(d \ln T / d \ln r)_{\text{conv}}$  depends on a cancellation between two terms of opposing signs (on the RHS of eq. [8]). At a density  $n_b \simeq n_{\text{sat}}$  and a density gradient  $d \ln \rho / d \ln r \simeq -3$ , the radiative temperature gradient becomes too weak to induce convection below a luminosity  $L_\nu \simeq 1 \times 10^{52} \text{ erg s}^{-1}$  and temperature of  $\sim 20 \text{ MeV}$ . Since the binding energy is  $3 \times 10^{53}$  ergs, the luminosity will be high enough to drive convection for 10 seconds or more.

Unlike a main sequence star, the thermal energy in the young neutron star is not generated in the central core. Heat is generated through the entire star as the lepton fraction relaxes to its equilibrium value. The absence of shock heating in the inner half of the star leads to a positive temperature gradient at small radii, which delays the onset of convection deep in the star (Burrows & Lattimer 1986). However, as the outer layers cool by neutrino loss, a negative entropy gradient is produced at smaller and smaller radii.

The above argument shows that passive neutrino transport through a newly formed neutron star leads inevitably to convective instability. Once the inconsistency of purely radiative heat transport is established, one knows that some fraction of the heat flux must be carried by convection. In other words, the negative entropy gradient is not entirely erased by the convection (as is apparent in the simulations of KJM). Rather, it is maintained at a large enough magnitude to carry the flux needed to supply that lost at the neutrinosphere – until the magnitude of the radiative gradient drops due to decreasing luminosity or increasing neutrino mean free path.

The convective energy flux is easily estimated using mixing length theory. In terms of the convective velocity  $V_{\text{con}}$ , one has

$$F_{\text{con}} \simeq \rho V_{\text{con}}^3. \quad (10)$$

Numerically,  $V_{\text{con}} \approx 10^8 \text{ cm s}^{-1}$ , which is much less than than the speed of light and substantially smaller than the sound speed  $c_s \approx 5 \times 10^9 \text{ cm s}^{-1}$ . Notice that the convective velocity varies as  $F_{\text{con}}^{1/3}$  and so depends weakly on the convective efficiency. As we review in

the next section, this means that *the maximum possible dynamo-generated magnetic field will also vary weakly with the convective efficiency.*

The latest numerical simulations reach differing conclusions about the persistence of Ledoux convection inside the  $\nu$ -sphere, but for reasons that can be ascribed in part to the handling of neutrino transport. KJM employ a fully two-dimensional hydrodynamic code, with neutrino transport restricted to radial rays, and find that convection continues over the entire Kelvin time. The simulations of Mezzacappa et al. (1998) further restrict neutrino transport to one spatial dimension, and find that the two-dimensional convective motions die out after a few tens of milliseconds. They argue that Ledoux convection is inhibited by neutrino transport in the outer layers of the neutron core ( $\rho \lesssim 10^{13} \text{ g cm}^{-3}$ ), where the diffusion time  $\sim \tau_{\nu_e} \ell_P / c$  is shorter than the convective overturn time in the absence of local neutrino heating and cooling. However, deeper in the core the convection overturn time  $\tau_{\text{con}} = \ell_P / V_{\text{con}} \sim 1 - 3 \text{ ms}$  is much shorter than the Kelvin time and this conclusion is reversed. The cooling models of Pons et al. (1999), which include more realistic neutrino opacities, find that a deep convective instability persists for tens of seconds.

A recent paper by Miralles, Pons, and Urpin (2000) carefully treats how convective instability is modified by the transport of heat and lepton number, and by viscosity. They find that the cooling neutron star simulated by Pons et al. (1999) is subject to a slower double-diffusive instability (the ‘neutron finger instability’; Wilson & Mayle 1988) even in regions that are stable according to the Ledoux criterion (1). Nonetheless, at both 1 s and 20 s, the region of the star that is subject to an unstable g-mode with a fast growth rate ( $\lesssim 1 \text{ msec}$ ; Fig. 3 of Miralles et al. 2000) closely approximates the region found previously to be unstable according to the Ledoux criterion (Fig. 24 of Pons et al. 1999). The new ‘convective’ instability criterion (eqs. [25] and [26] of Miralles et al. 2000) is more restrictive than Ledoux, so that regions of the star that are unstable according to eq. (1) are labelled as being subject only to the ‘neutron finger’ instability (in spite of the equally fast growth rate). In fact, one can show that this new ‘convective’ instability criterion remains more restrictive even in the limit of slow transport, where the Ledoux criterion should be accurate. For that reason, we interpret the results of Miralles et al. (2000) to imply that transport effects *do not* significantly restrict the region of a newborn neutron star that undergoes a vigorous convective instability.

## 2.2. Dynamical Balance between Convective and Magnetic Stresses

Even in the absence of rotation, these convective motions carry enough energy to amplify a magnetic field to enormous strengths. The argument for such a stochastic dynamo

is based on a *phenomenological scaling*, rather than purely theoretical considerations, and is presented in detail in TD93. One observes in the convective envelope of the Sun a small scale (‘intranetwork’) component of the magnetic field, with a mean pressure about 10 percent of the turbulent pressure,

$$\frac{\langle B^2 \rangle / 4\pi}{\rho V_{\text{con}}^2} \equiv \varepsilon_B \sim 0.1. \quad (11)$$

This field is present even at Solar minimum, when it is distributed almost uniformly across the Solar disk (Murray 1992). It has been conjectured to be the consequence of a stochastic, non-helical dynamo that builds up magnetic flux on the scale of an individual convective cell (TD93; Durney, de Young, & Roxburgh 1993). Such a dynamo would operate almost independently of the global Solar dynamo that manifests itself at the surface in the form of sunspot activity and the dipolar magnetic field<sup>2</sup>. Some theoretical support for this conjecture comes from models of dynamo action in mirror symmetric turbulence (Ruzmaikin & Sokoloff 1981; Meneguzzi & Pouquet 1989).

The total convective kinetic energy grows from  $E_{\text{con}} \sim 0.5$  to  $1 \times 10^{49}$  ergs between 0.1 and 1 s, as the convective zone expands to encompass the entire neutron star (KJM). At 0.1-0.2 s after bounce, a zone interior to  $0.9M_{\odot}$  is unstable to Ledoux convection, with overshoot extending out to an enclosed mass of  $1.05M_{\odot}$ . This is in accord with a simple mixing length argument (Burrows 1987; TD93). The convective luminosity is related to the luminosity  $L_{\nu} = L_{\nu 52} \times 10^{52}$  erg s<sup>-1</sup> in *all* neutrino species via  $L_{\text{con}} \sim L_{\nu} \sim 4\pi R_{\text{con}}^2 \rho V_{\text{con}}^3$ . The kinetic energy in convection  $E_{\text{con}} = \frac{4\pi}{3} R_{\text{con}}^3 \times \frac{1}{2} \rho V_{\text{con}}^2$  can then be expressed in terms of the convective overturn time

$$\tau_{\text{con}} \equiv \ell_P / V_{\text{con}} = 2 \times 10^{-3} \left( \frac{R_{\text{con}}}{30 \text{ km}} \right) \left( \frac{V_{\text{con}}}{3 \times 10^8 \text{ cm s}^{-1}} \right)^{-1} \text{ s} \quad (12)$$

via

$$E_{\text{con}} = L_{\text{con}} \tau_{\text{con}} \sim \left( \frac{1}{2} - 1 \right) \times 10^{50} \left( \frac{L_{\nu 52}}{5} \right) \left( \frac{\tau_{\text{con}}}{2 \text{ ms}} \right) \text{ ergs.} \quad (13)$$

The pressure scale height  $\ell_P \sim R/5$  while the nucleons are only mildly degenerate. Note that the convective overturn time is short compared with the expected initial spin periods of most neutron stars (Duncan & Thompson 1992). Applying the scaling (11) for the

---

<sup>2</sup>The two dynamos are not, of course, entirely independent: the global dynamo feeds magnetic flux into the convection zone. However, one infers from the time-variation of Solar p-mode frequencies with Solar cycle that the proportionality between magnetic and turbulent stresses is maintained down to at least six pressure scaleheights below the photosphere (Goldreich et al. 1991). This strongly indicates a local amplification mechanism that leads to a dynamical balance between the two stresses.

magnetic energy implies a total magnetic energy

$$E_B \equiv \int^{R_\nu} \frac{B^2}{8\pi} d^3x = \varepsilon_B E_{\text{con}} \sim 10^{49} \left( \frac{\varepsilon_B}{0.1} \right) \left( \frac{E_{\text{con}}}{10^{50} \text{ ergs}} \right) \text{ ergs} \quad (14)$$

inside the  $\nu$ -sphere. The corresponding r.m.s. magnetic field is

$$\langle B^2 \rangle_{R_\nu}^{1/2} = \left( \frac{6E_B}{R^3} \right)^{1/2} \sim 1.5 \times 10^{15} \left( \frac{\varepsilon_B}{0.1} \right)^{1/2} \left( \frac{E_{\text{con}}}{10^{50} \text{ ergs}} \right)^{1/2} \left( \frac{R_\nu}{30 \text{ km}} \right)^{-3/2} \text{ G.} \quad (15)$$

It should be noted that this dynamo process taps the energies of the diffusing  $\nu_\mu$  and  $\nu_\tau$ , as well as the  $\nu_e$ ,  $\bar{\nu}_e$ . By contrast, direct neutrino heating outside the  $\nu$ -sphere is mediated by absorption of  $\nu_e$  and  $\bar{\nu}_e$  only.

The region below the shock provides a second potential site for magnetic field amplification. Heating by the outward flux of electron-type neutrinos, through the charged-current absorption  $\nu_e(\bar{\nu}_e) + n(p) \rightarrow e^-(e^+) + p(n)$ , induces strong convection (e.g. Burrows et al. 1995; Janka & Muller 1996). The conditions are especially favorable for magnetic field amplification if prolonged infall continues after the shock succeeds (leading to the formation of a secondary accretion shock) or if the expansion of the shock is asymmetric, so that accretion continues in one hemisphere even as the shock expands in the opposing hemisphere (T00). Buoyancy forces will pin magnetized material just below the shock even while heavier material settles below the shock toward the neutrinosphere. The convective Mach number is expressed in terms of the accretion rate  $\dot{M}$ , shock radius  $R_{\text{sh}}$ , core mass  $M_{\text{core}}$ , and the (normalized) electron neutrino luminosity  $\mathcal{L} = Y_n L_{\bar{\nu}_e} (\langle \varepsilon_{\bar{\nu}_e}^2 \rangle / 200 \text{ MeV}^2) + Y_p L_{\nu_e} (\langle \varepsilon_{\nu_e}^2 \rangle / 200 \text{ MeV}^2)$ ,

$$(Ma)_{\text{con}} = 0.6 \varepsilon_{\text{heat}}^{1/3} \left( \frac{\mathcal{R}}{10} \right)^{1/2} \left( \frac{R_{\text{sh}}}{100 \text{ km}} \right)^{-1/6} \left( \frac{\mathcal{L}_{52}}{4} \right)^{1/3} \left( \frac{M_{\text{core}}}{1.4 M_\odot} \right)^{-1/2}. \quad (16)$$

Here  $\varepsilon_{\text{heat}}$  is the dimensionless ratio of the net heating rate (from which cooling by electron and positron captures has been subtracted) to the gross heating rate (uncompensated by neutrino cooling). The convective overturn time is  $\tau_{\text{con}} \simeq 2 \times 10^{-3} \varepsilon_{\text{heat}}^{-1/3} (R_{\text{sh}}/100 \text{ km})^{5/3} (\mathcal{L}_{52}/4)^{-1/3} \text{ s}$  (§2.3 of T00). This overturn is fast enough to allow many efoldings of the buoyant magnetic field, if the shock radius  $R_{\text{sh}}$  has collapsed to  $\sim 100 \text{ km}$ . When the magnetic stresses reach a dynamical balance with the convective stresses, according to equation (11), the strength of the field has increased to (T00)

$$\langle B^2 \rangle^{1/2} = 1 \times 10^{14} \varepsilon_{B-1}^{1/2} \varepsilon_{\text{heat}}^{1/3} \left( \frac{\dot{M}}{M_\odot \text{ s}^{-1}} \right)^{1/2} \left( \frac{R_{\text{sh}}}{100 \text{ km}} \right)^{-17/12} \left( \frac{\mathcal{L}_{52}}{4} \right)^{1/3} \left( \frac{\mathcal{R}}{10} \right)^{1/2} \left( \frac{M_{\text{core}}}{1.4 M_\odot} \right)^{3/4}. \quad (17)$$

### 2.3. Convective Dynamo During Late Infall

It is also worthwhile estimating how this equipartition field will diminish, as the rate of accretion drops off. Late infall ( $\Delta M = O(10^{-1}) M_\odot$  over  $\sim 10^3 - 10^4$  s) is a plausible consequence of the formation of a rarefaction wave in the exploding supernova core (Woosley & Weaver 1995; Fryer, Colgate, & Pinto 1999). Let us suppose that  $\dot{M}$  remains large enough that neutrino cooling at the base of the accretion flow continues to be dominated by electron/positron captures on free protons and neutrons, as compared with  $e^\pm$  annihilation  $e^+ + e^- \rightarrow \nu + \bar{\nu}$  (as assumed in the models of Chevalier 1989). We focus on the inner regions of the flow,  $R \sim 30 - 100$  km, well inside the accretion shock. Here the temperature is high enough for helium to be photo-dissociated, but the capture rates on free  $n, p$  are still small enough to prevent the formation of a stabilizing gradient  $dY_e/dR$ . The thermal pressure is then dominated by photons and (at least mildly) relativistic  $e^\pm$  pairs,  $P = \frac{11}{12}aT^4$ . The corresponding isentropic hydrostatic profile is  $T(R) \propto R^{-1}$ ,  $\rho(R) \propto R^{-3}$ , and  $P(R) \simeq \frac{1}{4}(GM_{\text{NS}}/R)\rho(R) \propto R^{-4}$ . The base of this settling flow may be defined as the radius where the flow time  $(\frac{1}{4}R/V_R)_R$  across a pressure scale-height equals the time  $(3P/\dot{Q}^{eN})_R$  for  $e^\pm$  captures to remove the thermal energy. (The neutrino emissivity per unit volume scales as  $\dot{Q}^{eN} \propto T^6 \rho$  in a medium with non-degenerate electrons.) Cooling is slower than advection outside this radius, and the gradient  $dY_e/dR$  is too weak to stabilize the flow against the effects of neutrino heating (Mezzacappa et al. 1998). As a result the flow becomes violently convective.

Combining the constraint of mass conservation,  $\dot{M} = 4\pi R^2 V_R \rho$ , with the equation of hydrostatic balance at the base of the settling flow, and taking the cooling radius to be a fixed multiple of the stellar radius<sup>3</sup>, one finds the scaling relations

$$\rho(R) \propto \dot{M}^{2/5}; \quad T(R) \propto \dot{M}^{1/10} \quad (18)$$

at a fixed radius  $R$ .

From the relations (18), one can deduce several things:

1. The temperature at the base of the settling flow typically exceeds  $m_e c^2$ , for parameters of interest, as is needed for the pressure to be dominated by photons and relativistic  $e^\pm$  pairs. For example, the temperature is  $\sim 1$  MeV at the base of an accretion flow carrying a mass flux  $\dot{M} \sim 10^{-4} M_\odot \text{ s}^{-1}$ .

2. The nucleons in the settling flow become less degenerate with decreasing accretion

---

<sup>3</sup>In the presence of an extended atmosphere, the stellar radius is conveniently defined as the radius where  $\rho = \rho_{\text{sat}}$ .

rate: the ratio of temperature to fermi energy scales as  $k_B T / \varepsilon_p \propto \dot{M}^{-1/6}$ . At the same time, the thermal energy per baryon remains almost constant at fixed radius,  $T^4 / \rho \propto \dot{M}^0$ , and so effective dissociation of helium is expected at the base of the accretion flow, even at relatively low accretion rates.

3. At an intermediate infall rate  $\sim 10^{-4} - 10^{-5} M_\odot \text{ s}^{-1}$ , the assumption of neutrino cooling by  $e^\pm$  captures is indeed self-consistent (as compared with  $e^\pm$  annihilation  $e^+ + e^- \rightarrow \nu + \bar{\nu}$ ). The relative rates of energy loss through these two channels vary weakly with  $\dot{M}$  at a fixed radius. In particular,  $\dot{Q}^{eN} / \dot{Q}^{e^\pm} \propto \rho / T^3 \propto \dot{M}^{1/10}$ , before  $e^\pm$  captures have removed enough heat to make the electrons degenerate.

4. Neutrino heating still causes the infalling material to be violently convective, before finally settling onto the neutron star surface (T00). At late times, the luminosity in electron-type neutrinos can be directly related to  $\dot{M}$ ,

$$L_{\nu_e} + L_{\bar{\nu}_e} = \frac{G \dot{M} M_{\text{NS}}}{R_{\text{NS}}} = 7 \times 10^{49} \left( \frac{\dot{M}}{10^{-4} M_\odot \text{ s}^{-1}} \right) \left( \frac{M_{\text{NS}}}{1.4 M_\odot} \right) \left( \frac{R_{\text{NS}}}{10 \text{ km}} \right)^{-1} \text{ ergs}^{-1}. \quad (19)$$

The heating rate (per unit volume) due to charged-current absorption of these neutrinos on the settling baryons is  $3P / \tau_{\text{heat}} \propto \rho \dot{M}$  (eq. [27]). The energy density in the resulting convective motions scales as  $\frac{1}{2} \rho V_{\text{con}}^2 \simeq (3P / \tau_{\text{heat}}) \times (\ell_P / V_{\text{con}})$ . As a result, the convective speed decreases more slowly with decreasing accretion rate,  $V_{\text{con}}(R) \propto \tau_{\text{heat}}^{-1/3} \propto \dot{M}^{1/3}$ , than does the settling speed,  $V_R(R) \propto \dot{M}^{3/5}$ . Moving outward through the accretion flow, the capture (cooling) timescale grows as  $\sim \rho^{-1} T^{-2} \sim R^5$ , given an approximately isentropic hydrostatic profile  $T \propto R^{-1}$  and  $\rho \propto R^{-3}$ . By contrast, the heating time increases only as  $\tau_{\text{heat}} \sim R^2$ . Thus, on general grounds one expects a ‘gain region’, within which  $dS/dR$  is strong enough, and  $dY_e/dR$  is weak enough, to trigger convection (e.g. Burrows et al. 1995; Janka & Muller 1996).

5. Finally, using the above scaling relations, it is easy to work out how the equipartition magnetic field scales with accretion rate:

$$\langle B^2 \rangle^{1/2} = \varepsilon_B^{1/2} (4\pi\rho)^{1/2} V_{\text{con}} \propto \dot{M}^{8/15}, \quad (20)$$

at a fixed radius. The equipartition field drops by a factor  $\sim 0.01$  from  $\dot{M} = 1 M_\odot \text{ s}^{-1}$  to  $\dot{M} = 10^{-4} M_\odot \text{ s}^{-1}$ .

### 3. Transport of Magnetic Fields

We now discuss the transport of a magnetic field through the convective interior and convectively stable exterior of a nascent neutron star. The star’s convective core is

surrounded by an overshoot layer of thickness  $\Delta M \sim 0.1M_\odot$  and another convectively stable layer of similar mass that extends out to the gain radius (KJM). Magnetic fields amplified in the convective region are transported rapidly into an adjoining overshoot layer (with a velocity  $\sim V_{\text{con}}/\ell_P$ ). Recent simulations of magetoconvection (Tobias et al. 1998) show the the magnetic field will remain pinned at the base of a convective layer, even against the action of buoyancy forces. Thus, we expect the overshoot layer above the convective core of a neutron star to acquire magnetic fields as strong as those in the core. Transport of the magnetic field through the surrounding convectively stable layer is greatly aided by i) the concentration of the field into a dense fibril state and ii) rapid neutrino heating. We also discuss an additional subtlety involving turbulent pumping, driven by a radial gradient in the turbulent diffusivity.

### 3.1. Turbulent Pumping within Convective Zones

A nascent neutron star and a late-type main sequence star both are deeply convective. In the outermost convective layers of a main sequence star, the turbulent diffusivity *increases outward* due to the recombination of hydrogen, which buffers the decrease of temperature with decreasing density. By contrast, there are no similar ionization effects that enhance the neutrino scattering or absorption cross sections in a neutron star and, as we now show, the turbulent diffusivity

$$\chi = \frac{1}{3}V_{\text{con}}\ell_P \quad (21)$$

*decreases outward*. Once the  $\nu$ -sphere shrinks to  $\sim 15 - 20$  km, the pressure scale height with the surface layer of mildly degenerate nucleons scales with density as  $\ell_P = P/\rho g \propto \rho^{2/3}R^2/M(< R)$ , where  $M(< R)$  is the mass enclosed within radius  $R$ . Constancy of the convective energy flux implies that  $V_{\text{con}} \propto \rho^{-1/3}R^{-2/3}$ . Combining these two expressions yields

$$\chi \propto \frac{\rho^{1/3}R^{4/3}}{M(< R)}. \quad (22)$$

One sees that  $\chi$  decreases with radius in the outer part of the convection zone, where  $\rho$  decreases at almost constant  $R$  and  $M(< R)$ . A similar conclusion holds for the convective shell in between the gain radius and the shock.

A passive contaminant such as smoke, or a magnetic field, experiences a net drift velocity in the direction of *decreasing* turbulent diffusivity,  $\vec{V}_{\text{drift}} = -\vec{\nabla}(V_{\text{con}}\ell_P)$ , whose magnitude is comparable to the convective velocity,  $|V_{\text{drift}}| \sim V_{\text{con}}$ . Magnetic flux ropes are convected *downward* in the upper layers of the Solar convection zone, and their buoyant

rise to the surface is prevented, as long as  $V_{\text{drift}} \gtrsim (a/\ell_p)^{1/2} B/\sqrt{4\pi\rho}$  (e.g. Ruzmaikin & Vainshtein 1978). (Here  $2a$  is the width of the flux rope.) By contrast, the mean drift velocity is directed *upward* at the top of a neutron star convection zone, and the magnetic heating rate should be correspondingly higher. We emphasize that this effect is more pronounced if the flux ropes are tied together into a larger network, so that the stochastic motions of individual flux ropes within individual convective cells are suppressed with respect to the mean drift velocity.

A related effect, which has been studied in the context of Solar magnetism, involves the asymmetry between cold downdrafts and hot updrafts in a compressible, convective layer. In the Solar convection zone the downdrafts are much denser and narrower than the updrafts and, as a result, have a higher vorticity. Radiation-hydrodynamical simulations (Dorch & Nordlund 2000) show that the magnetic field lines are wound up in the downdrafts, and suggest a tendency for the field to be pumped toward the bottom of the convective layer. The convective region of a newly formed neutron star is, however, supported by the pressure of mildly degenerate neutrons, and is less compressible than the Solar atmosphere. Numerical simulations (KJM) suggest a greater symmetry between downdrafts and updrafts than is inferred for the Sun.

### 3.2. Transport Aided by a High Neutrino Flux

In this section, we examine how the buoyant transport of a magnetic field through a supernova core is facilitated by the intense neutrino flux out of the core. The neutrinos have two principal effects, which we examine in turn. The first involves heating of the non-degenerate material outside the  $\nu$ -sphere, which equilibrates the temperature between a flux tube and its surroundings, and allows the tube to rise buoyantly across a convectively stable layer. The second effect involves transport of a magnetic field through the degenerate neutron core after convection has stopped and the core has become stably stratified. In such a situation, the transport rate is determined by the speed with which the electron fraction returns to its beta-equilibrium value (Pethick 1992; Goldreich & Reisenegger 1992). Long after the neutron star has radiated most of its original heat, the rate of modified URCA reactions may be kept high by magnetic dissipation (Thompson and Duncan 1996). During the first few seconds of the life of a neutron star, direct URCA reactions are possible, and proceed at an extremely high rate dominated by charged current absorption of  $\nu_e$  and  $\bar{\nu}_e$  on free nucleons.

We now focus on the early stages of a supernova explosion, *before* the success of the shock, and the onset of a low density, neutrino-driven wind outside the  $\nu$ -sphere. The

calculation separates into two cases, depending on whether the pressure is dominated by nucleons or by radiation and relativistic pairs. Curvature and tension forces, discussed in §4, are now ignored and the rope is assumed to sit horizontally in a plane-parallel atmosphere.

### 3.2.1. A Nucleon Pressure-Dominated Zone Outside the Neutrinosphere

The outer atmosphere of a newly formed neutron star is convectively stable, with entropy and electron fraction both having positive radial gradients,  $dS/dR, dY_e/dR > 0$ . Free neutrons within this layer absorb electron neutrinos at the rate

$$\dot{E}_{\nu_e+n \rightarrow p+e^-} = \frac{390}{f} \left( \frac{L_{\nu_e 52}}{4} \right) \left( \frac{\langle \varepsilon_{\nu_e}^2 \rangle}{200 \text{ MeV}^2} \right) \left( \frac{R}{100 \text{ km}} \right)^{-2} \text{ MeV neutron}^{-1} \text{ s}^{-1} \quad (23)$$

(Bethe & Wilson 1985). The dependence on the mean square neutrino energy is derived from the weak interaction cross section. The expression for proton heating ( $\bar{\nu}_e + p \rightarrow n + e^+$ ) is obtained by replacing  $L_{\nu_e}$  and  $\langle \varepsilon_{\nu_e}^2 \rangle$  with  $L_{\bar{\nu}_e}$  and  $\langle \varepsilon_{\bar{\nu}_e}^2 \rangle$ . Here  $f \simeq \frac{1}{4}$  for isotropic emission at the  $\nu_e$ -sphere, increasing to  $f = 1$  further out where the neutrinos free stream. The net heating rate due to absorption of  $\nu_e/\bar{\nu}_e$  on free neutrons ( $Y_n$  per nucleon) and protons ( $Y_p$  per nucleon) is

$$\dot{Q}^{\nu N} = \left( Y_n \dot{E}_{\nu_e+n \rightarrow p+e^-} + Y_p \dot{E}_{\bar{\nu}_e+p \rightarrow n+e^+} \right) \frac{\rho}{m_n}, \quad (24)$$

per unit volume. Heating is compensated by neutrino cooling driven (primarily) by electron and positron captures, so that the net heating rate becomes  $\dot{Q}^{\nu N} + \dot{Q}^{eN} = \dot{Q}^{\nu N} [1 - (T/T_{\text{eq}})^6]$ . The equilibrium temperature is

$$k_B T_{\text{eq}} \simeq 2.35 f^{-1/6} \left( \frac{\mathcal{L}_{52}}{4(Y_n + Y_p)} \right)^{1/6} \left( \frac{R}{100 \text{ km}} \right)^{-1/3} \text{ MeV}. \quad (25)$$

Here, we define the convenient dimensionless parameter

$$\mathcal{L}_{52} \equiv Y_n L_{\nu_e 52} \left( \frac{\langle \varepsilon_{\nu_e}^2 \rangle}{200 \text{ MeV}^2} \right) + Y_p L_{\bar{\nu}_e 52} \left( \frac{\langle \varepsilon_{\bar{\nu}_e}^2 \rangle}{200 \text{ MeV}^2} \right). \quad (26)$$

The time for the temperature to relax to the equilibrium (25) is  $\tau_{\text{heat}} \sim (\frac{3}{2} \rho k_B T / m_n) / 6 \dot{Q}^{\nu N}$ , or

$$\tau_{\text{heat}} \simeq 6 \times 10^{-4} f \left( \frac{T_{\text{MeV}}}{4} \right) \left( \frac{R}{50 \text{ km}} \right)^2 \left( \frac{Y_n L_{\nu_e 52} + Y_p L_{\bar{\nu}_e 52}}{4} \right)^{-1} \left( \frac{\langle \varepsilon_{\nu_e}^2 \rangle}{200 \text{ MeV}^2} \right)^{-1} \text{ s}, \quad (27)$$

since the heat capacity is dominated by free nucleons. The factor of  $\frac{1}{6}$  arises from the  $T^6$  dependence of the  $e^\pm$ -capture cooling rate. The effectiveness of neutrino heating can be

measured by comparing  $\tau_{\text{heat}}$  with the dynamical time  $\tau_{\text{dyn}} = \ell_P/c_s \sim (R/5)(5k_B T/3m_n)^{-1/2}$ :

$$\frac{\tau_{\text{heat}}}{\tau_{\text{dyn}}} = 1.6 f T_4^{3/2} \left( \frac{R}{50 \text{ km}} \right) \left( \frac{Y_n L_{\nu_e 52} + Y_p L_{\bar{\nu}_e 52}}{4} \right)^{-1} \left( \frac{\langle \varepsilon_{\nu_e}^2 \rangle}{200 \text{ MeV}^2} \right)^{-1}. \quad (28)$$

This implies  $\tau_{\text{heat}} \lesssim \tau_{\text{dyn}}$  at the  $\nu$ -sphere ( $R_\nu \sim 50 \text{ km}$  at 0.1 ms, decreasing to  $R_\nu \sim 20 \text{ km}$  at 1 s; e.g. Mayle & Wilson 1989).

The nucleon pressure is suppressed inside a magnetic flux rope that is in pressure equilibrium with its surroundings (Fig. 2),

$$\frac{B^2}{8\pi} + \frac{\rho_M k_B T_M}{m_n} = \frac{\rho k_B T}{m_n}. \quad (29)$$

However, the pressure of the electrons is only weakly perturbed by the magnetic field when  $Y_e$  is small. The density is high enough that the electrons are moderately degenerate ( $\mu_e/T \gtrsim \pi$ ),

$$\rho \gg \frac{(k_B T)^3 m_n}{(\hbar c)^3 Y_p} = 2 \times 10^8 Y_p^{-1} T_{\text{MeV}}^3 \text{ g cm}^{-3}. \quad (30)$$

At a fixed radius, the equilibrium electron pressure is the result of a competition between absorption of  $\nu_e/\bar{\nu}_e$ ,

$$\frac{\partial n_e}{\partial t} \propto R^{-2} [L_{\nu_e} \langle \varepsilon_{\nu_e} \rangle n_n - L_{\bar{\nu}_e} \langle \varepsilon_{\bar{\nu}_e} \rangle n_p] \simeq R^{-2} L_{\nu_e} \langle \varepsilon_{\nu_e} \rangle \frac{\rho}{m_n} (1 - 2Y_e), \quad (31)$$

and the capture of (degenerate) electrons on nucleons,

$$\frac{\partial n_e}{\partial t} \propto -\mu_e^6 \rho \propto -Y_e^2 \rho^3. \quad (32)$$

The electron fraction therefore varies with density as

$$\frac{1 - 2Y_e}{Y_e^2} \propto \rho^2, \quad (33)$$

at fixed  $R$ . The decrease  $\Delta P_e$  in electron pressure accompanying a decrease  $\Delta \rho$  in density is small where  $Y_e \ll 1$ ;

$$\frac{\Delta P_e}{P_e} = \frac{4Y_e}{3(1 - Y_e)} \frac{\Delta \rho}{\rho}. \quad (34)$$

Furthermore,  $P_e$  is only a fraction of the nucleon pressure because  $Y_e$  is small where  $\rho$  is large:

$$\frac{P_e}{P_n + P_p} = \frac{Y_e \mu_e}{4k_B T} = 0.3 \left( \frac{\rho}{10^{12} \text{ g cm}^{-3}} \right)^{1/3} \left( \frac{T_{\text{MeV}}}{4} \right) \left( \frac{Y_e}{0.1} \right)^{4/3}. \quad (35)$$

We conclude that the flux rope is less dense than its surroundings,  $\rho_M < \rho$ , when its temperature rapidly equilibrates with its surroundings. Rapid neutrino heating,  $\tau_{\text{heat}} \lesssim \tau_{\text{dyn}}$ , brings the temperature inside the flux rope close to the ambient value,  $T_M \simeq T$ . The density deficit inside the rope is then  $\rho_M - \rho \simeq -\rho\beta_P$ , where

$$\beta_P = \frac{B^2}{8\pi nT}. \quad (36)$$

Balancing the buoyancy force (integrated over the cross-sectional area  $\pi a^2$  of the rope) against the drag force  $C_d \times 2aV_R^2$ , yields the equilibrium vertical speed

$$V_R = \left( \frac{\pi}{4C_d} \frac{a}{\ell_P} \right)^{1/2} \frac{B}{\sqrt{4\pi\rho}}. \quad (37)$$

(cf. Parker 1979).

The vertical speed  $V_R$  is determined by the rate of neutrino heating when  $\tau_{\text{heat}} \gtrsim \tau_{\text{dyn}}$ . The force balance  $\rho_M V_R^2/a \sim g(\rho - \rho_M)$  implies that the density is almost uniform,  $\rho_M \simeq \rho$ , and that there is a temperature deficit

$$T_M - T = -\beta_P T \quad (38)$$

inside the rope. As the rope moves upward,  $T_M$  changes due to neutrino heating (eq. [27]) and adiabatic cooling,

$$\frac{1}{T_M} \frac{dT_M}{dt} = -\frac{1}{\tau_{\text{heat}}} \frac{T_M - T_{\text{eq}}}{T_M} + (\gamma - 1) \frac{1}{\rho_M} \frac{d\rho_M}{dt}. \quad (39)$$

Note that it is the equilibrium temperature (25), rather than the ambient temperature  $T$ , that enters on the right side of (39). Combining the conditions of pressure equilibrium and flux conservation,  $B/\rho_M = \text{constant}$ , yields the following relation between time derivatives,

$$\frac{1}{T_M} \frac{dT_M}{dt} = \frac{1}{P} \frac{dP}{dt} - (1 + 2\beta_P) \frac{1}{\rho_M} \frac{d\rho_M}{dt}. \quad (40)$$

Equations (38), (39) and (40) together yield

$$\frac{1}{\tau_{\text{heat}}} \frac{\beta_P T_{\text{eq}} - (1 - \beta_P)(T - T_{\text{eq}})}{T_M} = \frac{1}{P} \frac{dP}{dt} - (\gamma + 2\beta_P) \frac{1}{\rho_M} \frac{d\rho_M}{dt} = (\gamma - 1) \frac{dS}{dt} - \frac{2\beta_P}{\rho_M} \frac{d\rho_M}{dt}, \quad (41)$$

where  $S$  is the entropy per baryon in units of  $k_B$ . The vertical rise time  $\ell_P/V_R$  of the rope is obtained by substituting  $d/dt \rightarrow V_R(d/dR)$  and  $\rho_M \simeq \rho$ ,

$$\frac{\ell_P}{V_R} = \tau_{\text{heat}} \frac{(1 - \beta_P)T}{\beta_P T_{\text{eq}} - (1 - \beta_P)(T - T_{\text{eq}})} \left( \frac{\ell_P}{R} \right) \left[ (\gamma - 1) \frac{dS}{d \ln R} - 2\beta_P \frac{d \ln \rho}{d \ln R} \right]. \quad (42)$$

In the marginally failed shock model of Janka & Mueller (1996) one finds  $dS/d \ln R \simeq +12$ ,  $d \ln \rho / d \ln R \simeq -4$ , and  $\ell_P / R \simeq \frac{1}{5}$  within the stably stratified layer outside the  $\nu$ -sphere at 100 ms after bounce. Thus,

$$\frac{\ell_P}{V_R} \simeq 1.6 \tau_{\text{heat}} \left( \frac{1 - \beta_P^2}{\beta_P} \right) \quad (43)$$

when  $T \simeq T_{\text{eq}}$ .

It is straightforward to see that the upward, buoyant rise of a closed loop of magnetic flux will continue through the convectively stable layer outside the  $\nu$ -sphere and reach the convective shell interior to the shock. We consider both cases  $\beta_P \ll 1$  and  $\beta_P \simeq 1$  in turn. In the first case, the radial transport time is limited by neutrino heating (eq. [43]) and scales as  $\beta_P^{-1} f T R^2 \propto \beta_P^{-1} f R$ . The radial dependence of  $\beta_P$  is obtained by noting that the density inside the loop scales as  $\rho_M \sim \rho$ , and the flux density as  $B \sim \rho_M^{2/3}$ . Thus,  $\beta_P = B^2 / 8\pi P \propto \rho^{4/3} / P \propto R^{-1/3}$  and (using the same scalings  $\rho \propto R^{-4}$  and  $P \propto R^{-5}$ ) the transport time increases with radius. At the inner boundary of the convective shell ( $R \sim 100$  km) the transport time is only  $\sim 1 \times 10^{-3} \beta_P^{-1} (L_{\nu_e 52} / 4)^{-1} (\langle \varepsilon_{\nu_e}^2 \rangle / 200 \text{ MeV}^2)^{-1}$  s.

Transport is even faster when  $\beta_P \simeq 1$ , since buoyancy is effective even in the absence of neutrino heating. Balancing  $B^2 / 8\pi = P$ , and making use of the vertical velocity (37) of a horizontal flux rope, one finds

$$\frac{\ell_P}{V_R} \propto \frac{R^{3/2} \rho^{1/2}}{P^{3/8}}. \quad (44)$$

This yields  $\ell_P / V_R \propto R^{11/8}$ , using the same scalings for  $P$  and  $\rho$ .

### 3.2.2. A Radiation Pressure-Dominated Zone Outside the Neutrinosphere

We now consider transport of a magnetic field through a convectively stable atmosphere whose pressure is dominated by relativistic pairs and photons. The zone just interior to the gain radius fits this description. The temperature of the settling flow exceeds the equilibrium value  $T_{\text{eq}}$  (eq. [25]), and neutrino cooling dominates heating. The pressure equilibrium condition becomes

$$\frac{B^2}{8\pi} + \frac{11}{12} a T_M^4 \simeq \frac{11}{12} a T^4. \quad (45)$$

In this situation, the nucleon density inside the flux rope is an independent variable, which determines the strength of the buoyancy force and the rate of neutrino heating. When  $T_M^4 \ll T^4$ , the equilibrium magnetic flux density decreases with radius as  $B \propto T^2 \propto R^{-2}$ . The density inside a rising, horizontal flux rope decreases according to  $\rho_M \propto B \propto R^{-2}$ . By

contrast, the density of the surrounding settling flow decreases much more rapidly — faster than  $\rho(R) \propto R^{-3}$  because the relativistic entropy per baryon ( $S \propto T^3/\rho$ ) increases with radius. Thus, a flux rope will traverse several pressure scale heights only if it starts off at a density well below that of the ambient settling flow. In such a situation, direct neutrino heating is not required to ensure buoyancy. In practice, an effective barrier to magnetic buoyancy is not expected during the first  $\sim 1$  s, because the flow remains radiation-pressure dominated only within a short distance below the gain radius.

Radiation pressure also has a significant effect on the equilibrium shape of a magnetic arcade with fixed endpoints. An arcade of magnetic flux, whose footpoints are separated by an angle  $\Delta\phi$ , will open to infinity when  $\Delta\phi$  exceeds the critical value (79) given below. This critical angle depends on the dimensionless parameter  $\tilde{\ell}_P \propto \rho T/P$  (eq. [70]), in such a way that the critical footpoint separation decreases as photons and pairs contribute more to the pressure.

### 3.3. Transport in a Convectively Stable Neutron Core

We now consider the transport of a magnetic field in the central neutron core, after the core has become convectively stable. The electrically charged particles (protons and electrons) are tightly coupled to the magnetic field on short timescales. Transport of these charged particles through the degenerate neutron fluid proceeds extremely slowly, and at high temperatures is limited by neutron-proton drag (Goldreich and Reisenegger 1992). As a result, the interior of a newborn neutron star is very nearly an ideal magnetofluid. For this reason, we consider the bulk hydrodynamical motion of an isolated rope of magnetic flux. As in the previous section, we neglect curvature and tension forces and assume plane parallel symmetry.

The neutron core becomes convectively stable as it cools because  $\beta$ -equilibrium value of  $Y_e$  has a negative gradient, and the density of cool degenerate matter decreases with decreasing  $Y_e$  (Reisenegger & Goldreich 1992; §A.4). This happens, at the latest, when the temperature drops sufficiently that neutrinos begin to escape directly from the core. A flux rope that starts out in  $\beta$ -equilibrium is less dense than the surrounding fluid; as it rises buoyantly, it falls out of  $\beta$ -equilibrium and its density equilibrates. We treat the neutrons, protons and electrons as three ideal, degenerate Fermi fluids. The departure from  $\beta$ -equilibrium is measured by the chemical potential imbalance

$$\Delta\mu = \mu_p^M + \mu_e^M - \mu_n^M. \quad (46)$$

In pressure equilibrium,

$$P_e^M + P_p^M + P_n^M + \frac{B^2}{8\pi} = P_e + P_p + P_n, \quad (47)$$

which can be rewritten as

$$\Delta\mu_e n_e + \Delta\mu_p n_p + \Delta\mu_n n_n + \frac{B^2}{8\pi} = 0 \quad (48)$$

when the magnetic pressure is a small fraction of the total pressure. (As before, the superscript  $M$  denotes the interior of the flux rope, and  $\Delta\mu_e = \mu_e^M - \mu_e$ , etc.) The condition of charge neutrality,  $n_e^M - n_p^M = n_e - n_p = 0$ , leads to the relation

$$2 \frac{n_e \Delta\mu_e}{\mu_e} = \frac{n_p \Delta\mu_p}{\mu_p}, \quad (49)$$

and the condition of neutral buoyancy,  $n_n^M + n_p^M = n_n + n_p$ , leads to

$$\frac{n_n \Delta\mu_n}{\mu_n} + \frac{n_p \Delta\mu_p}{\mu_p} = 0. \quad (50)$$

One solves for  $\Delta\mu$  by combining these three equations,

$$\Delta\mu = \left[ \frac{2\mu_n}{(1 - Y_e)\mu_e} - 1 \right] \frac{B^2}{8\pi n_e}. \quad (51)$$

This expression can be simplified further after observing that the shift in the charged particle density is related to  $\Delta\mu$  via

$$\Delta\mu = \frac{\mu_e}{3n_e} \left[ \frac{2\mu_n}{(1 - Y_e)\mu_e} - 1 \right] (n_p^M - n_p), \quad (52)$$

so that

$$\frac{n_p^M - n_p}{n_p} = \frac{\Delta Y_e}{Y_e} = \frac{3}{4} \frac{B^2}{8\pi P_e}. \quad (53)$$

This shift in the electron fraction is similar, in order of magnitude, to that induced by the Lorentz force acting on a homogeneous  $n - p - e$  plasma without gravity (Goldreich and Reisenegger 1992).

The vertical speed  $V_R$  of the flux tube is limited by the rate at which the charged particle density is driven to its  $\beta$ -equilibrium value by absorption of  $\nu_e$  and  $\bar{\nu}_e$  on free nucleons,

$$\frac{\partial Y_e}{\partial t} + V_R \frac{\partial Y_e}{\partial R} = \frac{\Gamma(\nu_e + n \rightarrow e^- + p) - \Gamma(\bar{\nu}_e + p \rightarrow e^+ + n)}{\rho/m_n}. \quad (54)$$

Here  $\Gamma$  is the rate per unit volume, so that

$$\Gamma(\nu_e + n \rightarrow e^- + p) - \Gamma(\bar{\nu}_e + p \rightarrow e^+ + n) = \langle \sigma_{\nu_e n} \rangle n_{\nu_e} n_n^M c - \langle \sigma_{\bar{\nu}_e p} \rangle n_{\bar{\nu}_e} n_p^M c. \quad (55)$$

In equilibrium,

$$\frac{\langle \sigma_{\nu_e n} \rangle n_{\nu_e}}{\langle \sigma_{\bar{\nu}_e p} \rangle n_{\bar{\nu}_e}} = \frac{n_p}{n_n} = \frac{Y_e}{1 - Y_e}, \quad (56)$$

and so

$$\begin{aligned} \Gamma(\nu_e + n \rightarrow e^- + p) - \Gamma(\bar{\nu}_e + p \rightarrow e^+ + n) &= \langle \sigma_{\nu_e n} \rangle n_{\nu_e} (n_n^M - n_n) c - \langle \sigma_{\bar{\nu}_e p} \rangle n_{\bar{\nu}_e} (n_p^M - n_p) c \\ &= Y_e^{-1} \langle \sigma_{\nu_e n} \rangle n_{\nu_e} c (n_n^M - n_n). \end{aligned} \quad (57)$$

Since  $\Delta Y_e / Y_e$  is assumed to be small, one can express  $V_R$  in terms of the gradient of the unperturbed electron fraction,

$$V_R \simeq \frac{\Gamma(\nu_e + n \rightarrow e^- + p) - \Gamma(\bar{\nu}_e + p \rightarrow e^+ + n)}{(dY_e/dR)\rho/m_n}. \quad (58)$$

Combining equations (53), (57) with (58), one obtains

$$\frac{V_R}{c} = \frac{3}{4Y_e} \left| \frac{d \ln Y_e}{d \ln R} \right|^{-1} (\langle \sigma_{\nu_e n} \rangle n_{\nu_e} R) \frac{B^2}{8\pi P_e}. \quad (59)$$

Note that  $\langle \sigma_{\nu_e n} \rangle n_{\nu_e} R = (n_{\nu_e}/n_n) \tau_{\nu_e} = 7 \times 10^{-4} \tau_{\nu_e} (T_{\text{MeV}}/20)^3 (n_n/n_{\text{sat}})^{-1}$ . In this expression,  $\tau_{\nu_e} = n_n \langle \sigma_{\nu_e n} \rangle R \simeq 10^4 (k_B T/20 \text{ MeV})^3$  is the absorption depth at 15 MeV  $\lesssim k_B T \lesssim 40$  MeV (cf. Fig. 7 of Reddy et al. 1998). Substituting these expressions into (59), one obtains

$$\frac{V_R}{c} \simeq 4 \times 10^{-9} \tau_{\nu_e} \left( \frac{B}{1 \times 10^{14} \text{ G}} \right)^2 \left( \frac{T_{\text{MeV}}}{20} \right)^3 \left( \frac{Y_e}{0.05} \right)^{-7/3} \left( \frac{n_n}{n_{\text{sat}}} \right)^{-7/3}. \quad (60)$$

At the Kelvin time of  $\sim 3$  s, the density is  $n_n \sim n_{\text{sat}}$  and the temperature is  $k_B T \sim 20$  MeV at an enclosed mass of  $\sim 1 M_\odot$  (Fig. 9 of Pons et al. 1999). A flux rope is able to overcome the stable stratification from this depth only if  $V_R/c \gtrsim \frac{1}{3} R_{\text{ns}}/ct \sim 3 \times 10^{-6}$ , where  $R_{\text{ns}} \sim 10$  km is the stellar radius. The *lower* bound on the flux density which can rise buoyantly is then

$$B \gtrsim 3 \times 10^{13} \left( \frac{T_{\text{MeV}}}{20} \right)^{-3} \left( \frac{t}{3 \text{ s}} \right)^{-1/2} \text{ G}. \quad (61)$$

Notice the strong dependence on  $T$ . The direct URCA reactions freeze out at temperatures below  $k_B T \sim 10$  MeV, and so transport of the magnetic field to the stellar surface becomes ineffective at  $t \gtrsim 10$  s.

The net effect of this transport process is to exchange a region of high flux density with a region of lower flux density that lies above it. Over such short timescales, the neutron

matter moves with the magnetic field. A field that uniformly threads the neutron core does not induce buoyancy forces and can exceed (61). Perhaps coincidentally, this bound is comparable to the dipole magnetic field inferred for the Soft Gamma Repeater sources in the magnetar model (Thompson and Duncan 1996; Kouveliotou et al. 1999).

#### 4. Magnetostatic Equilibria

The convective core of a neutron star is surrounded by a convectively stable layer that extends from large to small neutrino optical depth, and straddles the neutrinospheres (Fig. 1). A rope of magnetic flux that is forced from below by convective overshoot into this layer can continue to rise buoyantly above the neutrinosphere, through the effects of neutrino heating as discussed in §3. We now consider the equilibrium shape of such a rope when its two endpoints are pinned from below (Fig. 3). The picture of the magnetic field that we adopt is one of spatially intermittent fibrils that are confined near the boundaries of convective cells below the  $\nu$ -sphere. Such a distribution is observed at the Solar photosphere (Stenflo 1989) and is inferred in the upper convection zone from helioseismology (Goldreich et al. 1991). It is also observed in simulations of a turbulent, conducting fluid at high magnetic Reynolds number (Thelen & Cattaneo 2000).

Aside from its dramatically higher temperature and stronger gravity, the exterior of newly formed neutron star is distinguished from the non-thermal atmosphere of the Sun in an important respect. Before the shock succeeds, the pressure remains high enough that magnetic flux originating inside the star will be confined to narrow fibrils well *outside* the  $\nu$ -sphere. To see this, we compare the pressure in the r.m.s. magnetic field (15) inside the  $\nu$ -sphere, with the pressure of free nucleons near the  $\nu$ -sphere,

$$\langle\beta\rangle = \frac{\langle B^2 \rangle_{R\nu}/8\pi}{nk_B T} = .005 \left(\frac{\varepsilon_B}{0.1}\right) \left(\frac{\rho}{10^{12} \text{ g cm}^{-3}}\right)^{-1} \left(\frac{T_{\text{MeV}}}{4}\right)^{-1} \left(\frac{R_\nu}{50 \text{ km}}\right)^{-3}. \quad (62)$$

This low volume average of  $\beta$  originates in the relatively low convective Mach number of the supernova core (as compared with the upper convection zone of the Sun), combined with the assumption of a common dynamo efficiency  $B^2/4\pi\rho V_{\text{con}}^2$ .

The field that pierces the  $\nu$ -sphere is not force free. We now calculate the equilibrium shape of a flux rope that is underdense compared with its surroundings and confined by the external pressure, so that  $B^2/8\pi \simeq P$ . The diameter of such a confined bundle of flux (of cross-sectional area  $\pi a^2$ ) increases slowly with distance  $R$  from the center of the neutron core,

$$\frac{a}{R} \propto R^{\beta/4-1} \sim R^0 - R^{1/4}, \quad (63)$$

since the pressure stratification outside the  $\nu$ -sphere is  $P(R) \propto R^{-\beta}$  ( $\beta \sim 4 - 5$ ).

As a result, the pressure scale height is a much larger fraction of the radius,  $\ell_P/R \sim \frac{1}{5}$ , near the  $\nu$ -sphere of a nascent neutron star, than it is near the Sun's photosphere, where  $\ell_P/R_\odot \sim 10^{-4}$ . As a result, a magnetic flux rope is subject to a strong buoyancy force on *both* sides of the  $\nu$ -sphere. To calculate the equilibrium shape of the rope, we first consider the case of a plane-parallel atmosphere. A flux rope sitting in the  $x - z$  plane (Fig. 3), with tangent vector

$$\hat{\mathbf{l}} = \cos \theta \hat{\mathbf{x}} + \sin \theta \hat{\mathbf{z}}, \quad (64)$$

is subject to a buoyancy force density

$$(\rho_M - \rho)\mathbf{g} = \beta_P \rho |g| \hat{\mathbf{r}}, \quad (65)$$

where

$$\beta_P \equiv \frac{B^2}{8\pi P} \quad (66)$$

and  $\rho_M$  is the density inside the flux rope. In equilibrium, the normal component of (65),

$$(\rho_M - \rho) [\mathbf{g} - (\mathbf{g} \cdot \hat{\mathbf{l}})\hat{\mathbf{l}}], \quad (67)$$

is balanced against the (normal) tension force density

$$\frac{B^2}{4\pi} \frac{\partial \hat{\mathbf{l}}}{\partial l}. \quad (68)$$

When neutrino heating equilibrates the temperatures inside and outside the flux rope (§3.2), the trajectory of the rope obeys the simple equation,

$$\frac{d\theta}{dl} = -\frac{\rho g}{2P_m} \cos \theta = -\frac{\cos \theta}{2\ell_P} \left( \frac{P}{P_m} \right). \quad (69)$$

Here  $P$  is the total pressure, and  $P_m = \rho T/m_n$  is the pressure in free nucleons (assuming that  $T > 1$  MeV and alpha particles are absent). A related expression has been written down by Parker (1979) for a plane-parallel atmosphere with negligible pressure in relativistic particles. The main consequence of the pairs and photons is to reduce the scale height from  $\ell_P = P/\rho g$  to

$$\tilde{\ell}_P = \frac{P_m}{\rho g} = \left( \frac{P_m}{P} \right) \ell_P. \quad (70)$$

The separation between the two footpoints is

$$\Delta x = \int \cos \theta dl = 2 \int_{-\theta_0}^{\theta_0} \tilde{\ell}_P[l(\theta)] d\theta, \quad (71)$$

and the maximum height attained by the arcade is

$$z_{\max} = 2 \int_0^{\theta_0} \tan \theta \tilde{\ell}_P[l(\theta)] d\theta, \quad (72)$$

where  $\theta_0$  is the inclination of the flux tube from the horizontal at  $z = 0$ . In an atmosphere with constant pressure scale height  $\tilde{\ell}_P$ , these expressions simplify to

$$\Delta x = 2\tilde{\ell}_P\theta_0 \leq 2\pi\tilde{\ell}_P, \quad (73)$$

and

$$z_{\max} = 2\tilde{\ell}_P \ln \left( \frac{1}{\cos \theta_0} \right). \quad (74)$$

The flux arcade expands to infinity as the footpoint separation approaches the critical value

$$\Delta x_c = 2\pi\tilde{\ell}_P, \quad (75)$$

at which the flux segments become vertical,  $\theta_0 = \frac{\pi}{2}$ . A similar effect will occur in any stably stratified, plane parallel atmosphere.

Notice that radiation pressure can have a significant effect on the equilibrium shape of a magnetic arcade, since  $\tilde{\ell}_P \propto \rho T/P$ . As a result, the critical footpoint separation decreases as photons and pairs contribute more to the pressure.

These results are easily generalized to an atmosphere with spherical symmetry. The shape of a flux arcade that sits in the equatorial plane (with azimuthal angle  $\phi$ ) is defined by the equation

$$\frac{d}{dl} (\theta - \phi) = -\frac{\cos \theta}{2\tilde{\ell}_P}, \quad (76)$$

which simplifies to

$$\frac{d\theta}{d\phi} = -\left( \frac{R}{2\tilde{\ell}_P} - 1 \right). \quad (77)$$

In a spherical atmosphere with  $\tilde{\ell}_P/R$  a constant, the flux arcade attains a maximum radius

$$R_{\max} = R_\nu \left( \frac{1}{\cos \theta_0} \right)^{(R/2\tilde{\ell}_P - 1)^{-1}}, \quad (78)$$

and opens to infinity when the angular separation between the footpoints approaches the critical value

$$\Delta\phi_c = \frac{2\theta_0}{R/2\tilde{\ell}_P - 1} = \frac{\pi}{R/2\tilde{\ell}_P - 1}. \quad (79)$$

For example, if the pressure is dominated by relativistic particles then  $\ell_P \simeq R/4$  and  $\tilde{\ell}_P$  is determined by the post-shock entropy. Substituting  $\tilde{\ell}_P \simeq R/5$  outside the  $\nu$ -sphere (around 100 msec after bounce), one deduces a critical separation

$$\Delta\phi_c \simeq \frac{2\pi}{3}. \quad (80)$$

Magnetic arcades that extend beyond the  $\nu$ -sphere are not fixed in position: their footpoints can be expected to wander in response to the convective motions below. Since these footpoint motions occur on the short timescale  $\sim \tau_{\text{con}}$ , it is important to check whether an individual arcade is able to reach a new equilibrium configuration over the timescale  $\sim \tau_{\text{con}}$ . Otherwise, the magnetostatic approximation is not justified. The motion of the upper part of an arcade is driven by the tension force  $f_{\text{tension}} = (\pi a^2)(B^2/8\pi R_c)$  (where  $R_c$  is the curvature radius and  $\pi a^2$  the cross-section of the flux rope) and is resisted by the hydrodynamical drag force  $f_{\text{drag}} = 2C_d a \rho V^2$ . Given a footpoint separation  $\sim 2R_c$ , the velocity of the rope (unimpeded by drag) is  $V \sim 2R_c/\tau_{\text{con}}$ , and the ratio of drag to tension forces is

$$\frac{f_{\text{drag}}}{f_{\text{tension}}} = 0.6 \frac{1}{\beta_P} \left(\frac{R}{50 \text{ km}}\right)^2 \left(\frac{T_{\text{MeV}}}{4}\right)^{-1} \left(\frac{2R_c}{\ell_P}\right)^2 \left(\frac{\tau_{\text{con}}}{3 \text{ ms}}\right)^{-2} \left(\frac{a}{0.5R_c}\right)^{-1}. \quad (81)$$

One sees that smaller flux arcades ( $2R_c \sim \ell_P$ ) that sit near the  $\nu$ -sphere ( $R_\nu \sim 30 - 50 \text{ km}$ ) will be able to follow the footpoint motions, whereas larger arcades that extend to a radius  $R \gg R_\nu$  will lag behind, and probably become very tangled.

Self-reconnection is also possible for smaller flux arcades that expand into the convective layer that sits below the shock; or for those which rotate rigidly with the central neutron star and experience a ram pressure force density

$$\rho(R)(\Omega_{\text{core}}R)^2 \quad (82)$$

that exceeds the buoyancy force density (65). This second condition is satisfied beyond a radius

$$R_{\text{max}} = 320 \left(\frac{P_{\text{core}}}{100 \text{ ms}}\right)^{2/3} \left(\frac{M_{\text{core}}}{M_\odot}\right)^{1/3} \left(\frac{\rho - \rho_M}{\rho}\right)^{1/3} \text{ km}, \quad (83)$$

where  $P_{\text{core}} = 2\pi/\Omega_{\text{core}}$  is the rotation period of the neutron core. However, as discussed in Chevalier (1989) and Thompson (2000), the neutron star may acquire its rotational angular momentum only during the last stages of accretion from the pre-supernova core.

## 5. Implications for Pulsars

This paper has investigated the response of a magnetic field to the violent fluid motions and intense neutrino flux within a supernova core. We can summarize our conclusions as follows:

1. Two principal sources of free energy are available for amplifying a magnetic field in a non-rotating supernova core: the violent convection occurring within the neutrinosphere (TD93); and within the gain region in between the neutrinosphere and shock (T00). The equilibrium magnetic field in these two convective zones is respectively  $\sim 10^{15}$  and  $\sim 10^{14}$  G (eqs. [15] and [17]). The convection occurring within the neutrinosphere is a robust consequence of the diffusive transport of heat by neutrinos (Appendix A). Even during relatively late fall-back ( $\sim 0.1 M_{\odot}$  over  $\sim 10^3$  s), the neutrino flux is high enough to induce vigorous convection within the material below the accretion shock.

2. The supernova core also contains regions which are stable to Ledoux convection, including the material which straddles the neutrinosphere(s). The transport of magnetic fields across these regions is greatly facilitated by the absorption of electron-type neutrinos (and anti-neutrinos) on free neutrons (and protons). The field induces a chemical potential imbalance between electrons, neutrons, and protons (cf. Goldreich & Reisenegger 1992), but the charged-current reactions force this imbalance toward zero (§3). During the main Kelvin-Helmholtz cooling phase of a nascent neutron star, this process effectively transports material containing fields stronger than  $\sim 10^{13}$  G out of the star.

3. During periods of hyper-Eddington accretion, the equilibrium shape of a magnetic flux rope which protrudes across the neutrinosphere is strongly modified by the hydrostatic pressure of the settling material. In the case of a flux rope anchored at both ends, the resulting buoyancy force leads to a critical separation between the ends of the flux rope, above which the rope expands to very large radius (§4). This mechanism provides a means of feeding large amounts of magnetic flux from a dynamo operating within the neutrinosphere, to the neutrino-heated ‘gain region’ outside the neutron core. The interaction of this field with the accretion flow has been investigated elsewhere (T00).

Claims that late fallback will tend to bury a magnetic field (e.g. Geppert, Page, & Zannias 1999) should, as a result, be treated with caution. The full implications of these physical processes for pulsar magnetism (and perhaps also the supernova mechanism) can only be gleaned by incorporating them into full numerical simulations of the supernova collapse. The behavior of a centrifugally-supported accretion flow is, in particular, beyond the scope of this paper. Nonetheless, several qualitative conclusions will be summarized here, in the following sections.

### 5.1. Principal Phase of Dynamo Amplification

Both the gain region below the accretion shock and the interior of the neutron star are strongly convective. The ratio of convective kinetic energy to gravitational binding energy is a hundred times larger in the proto-neutron star phase, than during any previous convective phase driven by nuclear burning (TD93). It is even larger in the convective gain region below an accretion shock (T00). Since the ratio of magnetic energy to gravitational binding energy is approximately conserved during gravitational collapse, these violent fluid motions during the supernova event are expected to be the dominant source of free energy for pulsar magnetism. The relative importance of the two convective regions for the surface fields of radio pulsars, depends in part on the amount of fallback following the success of the supernova shock.

Even during late infall ( $10^3 - 10^4$  s after collapse) the settling flow is heated sufficiently to become violently convective. As reviewed in §2.2, the settling speed scales as  $V(R) \propto \dot{M}^{3/5}$  when cooling is dominated by  $e^\pm$  captures on free protons and neutrons, whereas the convective speed decreases more slowly,  $V_{\text{con}}(R) \propto \dot{M}^{1/3}$  (at fixed radius  $R$ ). The equipartition magnetic field within the flow scales as  $\langle B^2 \rangle^{1/2} \propto \dot{M}^{8/15}$  (eq. [20]).

### 5.2. Prompt Convective Dynamo and the Surface Magnetic Fields of Young Neutron Stars

The bulk of the crust of a neutron star is derived from material that is either processed through the convective shell below the accretion shock; or rises buoyantly from the deep interior of the neutron core through the convectively stable layer that straddles the  $\nu$ -sphere. The equilibrium flux density (17) in the outer convective shell, scaled to the density of the neutron star crust, is

$$B_{\text{crust}} \sim \left( \frac{\rho_{\text{sat}}}{\rho_2} \right)^{2/3} \langle B^2 \rangle^{1/2}, \quad (84)$$

or equivalently,

$$B_{\text{crust}} \sim 2 \times 10^{17} \left( \varepsilon_B \mathcal{R} \right)^{1/2} \left( \frac{\dot{M}}{M_\odot \text{ s}^{-1}} \right)^{-1/6} \left( \frac{R_{\text{sh}}}{100 \text{ km}} \right)^{-5/12} \left( \frac{\mathcal{L}_{52}}{4} \right)^{1/2} \left( \frac{M_{\text{core}}}{1.4 M_\odot} \right)^{13/12} \quad \text{G.} \quad (85)$$

Here  $\rho_2$  is the post shock density (eq. [16]). This field can be expected to be coherent on the small scale

$$\ell_B \sim \left(\frac{\rho_2}{\rho_{\text{sat}}}\right)^{1/3} \ell_P(R_{\text{sh}}) = 0.5 \left(\frac{R_{\text{sh}}}{100 \text{ km}}\right)^{-1/2} \left(\frac{\dot{M}}{1 M_\odot \text{ s}^{-1}}\right)^{1/3} \left(\frac{\mathcal{R}}{10}\right)^{1/3} \left(\frac{M_{\text{core}}}{1.4 M_\odot}\right)^{-1/6} \text{ km.} \quad (86)$$

This leads to a net dipole field

$$B_{\text{dipole}} \sim \langle B^2 \rangle^{1/2} \left(\frac{\ell_B^2}{4\pi R_\star^2}\right)^{1/2}, \quad (87)$$

namely

$$B_{\text{dipole}} = 3 \times 10^{15} \varepsilon_{B-1}^{1/2} \left(\frac{\dot{M}}{M_\odot \text{ s}^{-1}}\right)^{1/6} \left(\frac{R_{\text{sh}}}{100 \text{ km}}\right)^{-11/12} \left(\frac{\mathcal{L}_{52}}{4}\right)^{1/2} \left(\frac{\mathcal{R}}{10}\right)^{5/6} \left(\frac{M_{\text{core}}}{1.4 M_\odot}\right)^{11/12} \text{ G.} \quad (88)$$

A further multiplicative factor of  $(\ell_B/R_{\text{NS}})^{1/2} \sim (\rho_2/\rho_{\text{sat}})^{1/6}$  must be included if one also averages the dipole field through many radial shells of thickness  $\ell_B$ . This estimate applies to the field generated by convective motions in the outer part of the gain region.

Material that rises buoyantly past the  $\nu$ -sphere must also be strongly magnetized. The strong neutrino flux aids buoyancy forces, but the magnetized fluid will reach the surface of the star during the prompt Kelvin-Helmholtz phase, only if  $B > 10^{13}$  G (eq. [61]). Weaker magnetic fields that are more characteristic of the dipole fields of ordinary radio pulsars are not able to reach the neutrinosphere, and according to our current understanding of transport through the crust will remain buried for  $\sim 10^8$  yr or longer (e.g. Goldreich & Reisenegger 1992). This suggests that a prompt convective dynamo can explain the observed magnetic dipole fields of radio pulsars only if the dynamo operates stochastically – generating a true dipole component through the incoherent superposition of stronger, small scale fields (TD93).

### 5.3. Effects of Late Fallback

Even after the shock is pushed to large radius, continuing fallback (driven by the formation of a reverse shock) can keep the hydrostatic pressure at the surface of the nascent neutron star well above the surface value of  $B^2/8\pi$  inferred for the dipole fields of young radio pulsars. For example, the hydrostatic pressure of a spherical shell of mass  $\Delta M$  corresponds to a field strength

$$B = \left(\frac{2GM_{\text{NS}}\Delta M}{R_{\text{NS}}^4}\right)^{1/2} = 3 \times 10^{17} \left(\frac{\Delta M}{0.1 M_\odot}\right)^{1/2} \left(\frac{M_{\text{NS}}}{1.4 M_\odot}\right)^{1/2} \left(\frac{R_{\text{NS}}}{10 \text{ km}}\right)^{-2} \text{ G.} \quad (89)$$

We focus here on the consequences of *spherical* accretion. (The behavior of a centrifugally supported flow may be substantially different, because it may not be able to maintain the large central cusp in the temperature and density needed to effect rapid neutrino cooling.)

Consider first the equipartition magnetic field which is maintained by the convective motions within the material settling onto the neutron star, driven by neutrino heating. At low accretion rates, the accretion shock lies at a large radius, and so it is appropriate to focus on a fixed radius  $R \lesssim 100$  km, where  $\langle B^2 \rangle^{1/2} \propto \dot{M}^{8/15}$  (eq. [20]). Allowing for an additional factor of  $\sim (\rho_{\text{sat}}/\rho)^{1/6}$  – relating the net dipole field to the equipartition field in the settling flow (§5.2) – one obtains the relation

$$B_{\text{dipole}} \propto \dot{M}^{7/15} \quad (90)$$

between the dipole field generated by convective fallback, and the rate of mass accretion. The estimate (88) then reduces to  $B_{\text{dipole}} \sim 10^{13}$  G at an accretion rate  $\dot{M} = 10^{-4} M_{\odot} \text{ s}^{-1}$ .

Next, we consider how the continuing flux of electron-type neutrinos will promote the buoyancy of magnetic fields which are anchored below the final layer of accreted material. We start with eq. (43) for the radial drift speed of a (horizontal) magnetic flux rope through an atmosphere of non-degenerate nucleons, given a heating rate (27) by charged-current absorption of  $\nu_e$  and  $\bar{\nu}_e$ . At an intermediate accretion rate  $10^{-1} \gtrsim \dot{M} \gtrsim 10^{-4}$ , the gravitational binding energy is carried off through  $e^{\pm}$  capture on free nucleons in the settling flow (T00), as compared with  $e^{\pm}$  annihilation at lower accretion rates (Chevalier 1989). The associated luminosity is directly related to  $\dot{M}$  by eq. (19). Making use of the scalings (18) of density and temperature with  $\dot{M}$  (at fixed radius within the settling flow), one finds that the nucleons become less degenerate as  $\dot{M}$  decreases. Magnetic flux poking out of the nascent neutron star will, as the result of buoyancy forces, carry with it a slightly lower mass density and maintain a similar degree of degeneracy to the surrounding flow.

It is now straightforward to derive the critical  $\beta_P = B^2/8\pi nT$  above which a parcel of magnetized fluid will rise buoyantly over the infall time  $\tau_{\text{infall}} \sim 10^3$  s. One obtains

$$\beta_P \gtrsim 1.6 \frac{\tau_{\text{heat}}}{\tau_{\text{infall}}} = 1 \times 10^{-5} \left( \frac{\dot{M}}{10^{-4} M_{\odot} \text{ s}^{-1}} \right)^{-11/10} \left( \frac{\tau_{\text{infall}}}{10^3 \text{ s}} \right)^{-1} \left( \frac{R_{\text{NS}}}{10 \text{ km}} \right)^3 \left( \frac{M_{\text{NS}}}{1.4 M_{\odot}} \right)^{-1} \quad (91)$$

from equations (27) and (43). The tiny numerical factor shows that the surface magnetic field almost certainly cannot be shielded diamagnetically by the accreted material ( $\Delta M \sim \dot{M} \tau_{\text{infall}}$ ), because in that circumstance  $\beta_P \gtrsim 1$ . Burial is possible only if the pre-existing magnetic field undergoes partial turbulent mixing with a fraction of the accreted material, so as to force  $\beta_P$  below the value (91).

#### 5.4. Origin of the Low-order Magnetic Multipoles of Neutron Stars

At least two distinct types of hydromagnetic dynamos can give rise to the dipole magnetic fields of neutron stars. The dipole field can either be amplified by fluid stresses that are coherent over a substantial fraction of the stellar radius (e.g. the classical  $\alpha - \Omega$  dynamo driven by a combination of rapid differential rotation and convection); or it can be built up by much smaller units that themselves are more strongly magnetized. In the convective interior of a neutron star, the first type of dynamo requires very rapid rotation,  $P \lesssim \ell_P/V_{\text{con}} \sim 3$  ms, and has been conjectured to result in magnetars with dipole fields in excess of  $10^{14}$  G. The second type of stochastic dynamo has been conjectured to generate the small scale, intranetwork magnetic field of the Sun (TD93; Durney, de Young, & Roxburgh 1993), but is ineffective at generating low order magnetic multipoles in a main sequence star. For example, the pressure scale height at the Solar photosphere is only  $\sim 10^{-4}$  of the Solar radius, which implies that the dipole flux density resulting from the incoherent superposition of the small scale dipoles is suppressed by a factor  $\sim (2\pi R_{\odot}^2/\ell_P^2)^{-1/2} \sim 10^{-4}$ . By contrast,  $\ell_P \sim R_{\text{ns}}/30$  at the neutrinosphere of a newly formed neutron star, during the last stages of Kelvin-Helmholtz cooling. The corresponding suppression factor is  $\sim 10^{-2}$ . This can comfortably accommodate the dipole fields of young radio pulsars, which characteristically lie in the range  $\sim 3 \times 10^{11} - 10^{13}$  G.

A similar stochastic dynamo may operate in the convective accretion flow onto a nascent neutron star. During *prompt* fallback, within  $\sim 1$  s after collapse, this mechanism could generate a dipole field as large as  $\sim 10^{14} - 10^{15}$  Gauss (eq. [88]). However, the equipartition magnetic field in the convective settling flow becomes weaker with increasing fallback time (and decreasing  $\dot{M}$ ; eq. [90]). This means that variability in the amount of fallback is an alternative explanation for the presence of a range of dipole fields in young neutron stars – with magnetars representing those objects with the smallest amount of late fallback. It is interesting to note that the current (uncertain) estimates of the mass accreted during late fallback ( $\Delta M \sim 0.03 - 0.1 M_{\odot}$ ; e.g. Fryer, Colgate, & Pinto 1999) typically exceed the mass of the rigid crust in model neutron stars ( $\sim 0.02 M_{\odot}$ ). As a result, the field generated during fallback will tend to be anchored in the neutron star core.

#### 5.5. Observational Tests of the Dynamo Mechanism

Given the extreme difficulty of inferring the initial spins of radio pulsars, models of the dynamo origin of pulsar magnetic fields are most tightly constrained by searches for correlations between  $\mathbf{B}$  and  $\mathbf{\Omega}$ . The stochastic dynamo does not depend in any way on rotation, and so predicts that these two vectors are randomly oriented with respect to

each other. By contrast, the magnetic field formed by a large-scale helical dynamo in a rapidly rotating neutron star should be strongly correlated with the rotation axis. In addition, a neutron star containing a toroidal magnetic field stronger than  $\sim 10^{14}$  G (and an external magnetic dipole that is approximately aligned with the symmetry axis of the internal field) has a tendency to reach an alignment between  $\mathbf{\Omega}$  and the external magnetic moment (cf. Goldreich 1971). This effect is more likely to induce alignment in the Soft Gamma Repeaters and Anomalous X-ray Pulsars, than in young radio pulsars (Duncan, Li & Thompson 1994).

### 5.6. Relaxation of Small-Scale Magnetic Fields

A small scale magnetic field of strength  $10^{14} - 10^{15}$  G in radio pulsars would be manifested through sudden fractures of the neutron star crust. This phenomenon could possibly play a role in triggering glitches (TD93) by intermittently heating the crust, or inducing rapid translations of the Coulomb lattice with respect to the neutron superfluid. Nonetheless, the absence of X-ray bursts associated with radio pulsars, combined with the seismic quiescence of old radio pulsars, suggests that if such a field is present it must be buried fairly deeply. Either a radio pulsar must have accreted upwards of  $\sim 10^{-2} M_{\odot}$  of *weakly* magnetized material ( $B \sim 10^{12} - 10^{13}$  G) following the brief dynamo epoch (eq. [90]), or the high order magnetic multipoles produced by convection were effectively smoothed out.

The stability of higher magnetic multipoles depends on the ability of the gravitationally stratified fluid to undergo fully three-dimensional motions (TD93). Stable stratification, which forces the fluid to move along the equipotential surfaces of the star, may allow more complicated magnetic topologies. However, we have shown that the absorption and emission of electron-type neutrinos facilitates the buoyant motion of magnetic fields as weak as  $\sim 10^{13} - 10^{14}$  G (during the prompt Kelvin-Helmholtz phase of a proto-neutron star), and so will facilitate the reconnection and unwinding of stronger fields.

### ACKNOWLEDGEMENTS

We gratefully acknowledge conversations with Phil Arras, Leon Mestel, Ewald Mueller, and Mal Ruderman. Financial support has been provided to both authors by the NSERC of Canada; and to C.T. by the Sloan Foundation.

### A. Convection in Young Neutron Stars

In this appendix we calculate the temperature gradient required to trigger convection in the presence of the stabilizing composition gradient found in a cooling neutron star. This gradient is derived below and given in eqn. (8) in the main text. We compare the result to that of Lattimer & Mazurek (1981), who find that lepton-fraction gradients tend to be stabilizing at low lepton fraction, and Reisenegger & Goldreich (1992), who find that the  $Y_e$ -gradient in a cold neutron star at  $\beta$ -equilibrium is absolutely stabilizing. The critical value of  $Y_l$ , below which the lepton gradient is stabilizing, increases at high temperatures and low densities, a result embodied in eqn. (A33) below. Although more detailed numerical cooling models are now available (e.g. Pons et al. 1999), the following arguments are useful for the physical insight they provide.

We are interested in the response of a neutron star to displacements of fluid elements. The temperature and density of the stellar material vary with radius; moving material radially will result in buoyancy forces which can either oppose or enhance the force initiating the displacement, depending on the thermodynamic state of the star. We assume that the star is in hydrostatic equilibrium, with equilibrium density and pressure gradients  $d\rho_0/dR$  and  $dP_0/dR$ , related by

$$\frac{dP_0}{dR} = -\rho_0 g \tag{A1}$$

and an equation of state

$$P = P(\rho, T, Y_e, Y_{\nu_e}). \tag{A2}$$

The density and temperature are assumed to be high enough that the stellar material is composed entirely of neutrons, protons, electrons, and neutrinos.<sup>4</sup> The relative proportions of these species are related to the total nucleon density<sup>5</sup>  $n_b = \rho/m_n$  by the parameters  $Y_e = (n_{e^-} - n_{e^+})/n_b$ ,  $Y_p = n_p/n_b = Y_e$  (from overall electric charge neutrality),  $Y_{\nu_e} = (n_{\nu_e} - n_{\bar{\nu}_e})/n_b$ , and  $Y_n = n_n/n_b = 1 - Y_e$ . The total lepton fraction is

$$Y_l = Y_e + Y_{\nu_e}. \tag{A3}$$

We model each species of particle as an almost degenerate, ideal fermi gas with chemical potential  $\mu_i$ . The background configuration is assumed to be in chemical equilibrium:

$$\mu_n + \mu_{\nu_e} = \mu_p + \mu_e. \tag{A4}$$

---

<sup>4</sup>But not so high that  $\mu$  and  $\tau$  leptons, pions, or strange particles are generated in significant abundances.

<sup>5</sup>We ignore the electron mass as well as the small mass difference  $m_n - m_p$ .

In a hot neutron star ( $T \gtrsim 10$  MeV), which is optically thick to all the neutrino species, a displaced fluid element can be assumed to remain in chemical equilibrium. At very high temperatures, the lepton fraction can also be assumed to be frozen into a buoyant plume of material,  $Y_i \simeq \text{constant}$ . The convective efficiency is significantly reduced once the optical depth  $\tau_{\nu_e}$  to electron neutrinos across a pressure scale height drops to a value  $\sim c/V_{\text{con}} \sim 300$ , where  $V_{\text{con}} \sim 10^8$  cm s $^{-1}$  is the speed of the convective overturns (cf. Mezzacappa et al. 1998). The corresponding mean free path to  $\nu_e + n \rightarrow p + e^-$  is  $\lambda \sim 10^3$  cm, which is reached at a temperature  $k_B T \sim 15$  MeV at nuclear saturation density ( $n_b = n_{\text{sat}} = 1.6 \times 10^{38}$  cm $^{-3}$ ; cf. Fig. 7 of Reddy et al. 1998). In fact, as we now show, this temperature is comparable to the value below which a purely radiative flux of neutrinos can be maintained without inducing convective instability.

### A.1. Convective Instability

We first review the derivation of the buoyancy force and the Brunt-Väisälä frequency  $N$  associated with the displacement of a fluid element from its equilibrium position. After a displacement through a distance  $\xi$  in the radial direction, the density of a fluid element becomes

$$\rho_d(R + \xi) = \rho(R) + \left( \frac{\partial \rho}{\partial R} \right)_{s, Y_i} \xi. \quad (\text{A5})$$

The subscripts indicate that the entropy and composition are held fixed in calculating the derivative.

The buoyancy force arises because this density differs from the background density at  $r + \xi$ :

$$\rho_0(R + \xi) = \rho(R) + \frac{d\rho_0}{dR} \xi. \quad (\text{A6})$$

The (Eulerian) density difference is

$$\delta\rho \equiv \rho_d(R + \xi) - \rho_o(R + \xi) \approx \left( \frac{d\rho}{dR} \right)_{s, Y_i} \xi - \frac{d\rho_0}{dR} \xi, \quad (\text{A7})$$

resulting in a buoyancy force

$$F_B = -g\delta\rho = -g \left[ \left( \frac{d\rho}{dR} \right)_{s, Y_i} - \frac{d\rho_0}{dR} \right] \xi \quad (\text{A8})$$

Suppose we move a bit of fluid upward, so that  $\xi > 0$ . If the density of the displaced fluid element is less than that of the surrounding material ( $\delta\rho < 0$ ) then the term inside the

square brackets in eqn. (A8) is negative. The buoyancy force is upward, in the direction of the original displacement, and the star is unstable to convection.

Young neutron stars have both entropy and composition gradients, so it is convenient to express the buoyancy force and  $N$  in terms of those gradients. Noting that  $\rho(R) = \rho[P(R), S(R), Y_l(R)]$  we find

$$\left(\frac{d\rho}{dR}\right)_{S,Y_l} = \left(\frac{\partial\rho}{\partial P}\right)_{S,Y_l} \frac{dP_0}{dR} \quad (\text{A9})$$

and

$$\left[\left(\frac{\partial\rho}{\partial P}\right)_{S,Y} \frac{dP_0}{dR} - \frac{d\rho_0}{dR}\right] = - \left[\left(\frac{\partial\rho}{\partial S}\right)_{P,Y} \frac{dS_0}{dR} + \left(\frac{\partial\rho}{\partial Y}\right)_{P,S} \frac{dY_{l,0}}{dR}\right]. \quad (\text{A10})$$

The condition for convective instability becomes

$$\left[\left(\frac{\partial\rho}{\partial S}\right)_{P,Y_l} \frac{dS_0}{dR} + \left(\frac{\partial\rho}{\partial Y_l}\right) \frac{dY_{l,0}}{dR}\right] > 0 \quad (\text{A11})$$

Since  $\left(\frac{\partial\rho}{\partial S}\right)_{P,Y_l} < 0$ , the condition for triggering convection is

$$\frac{dS_0}{dR} + \frac{(\partial\rho/\partial Y_l)_{P,S} dY_{l,0}}{(\partial\rho/\partial S)_{P,Y_l} dR} = \frac{dS_0}{dR} - \left(\frac{\partial S}{\partial Y_l}\right)_{P,\rho} \frac{dY_{l,0}}{dR} < 0, \quad (\text{A12})$$

which is eqn. (1) in the main text.

## A.2. Influence of a Compositional Gradient

The sign of the thermodynamic derivative  $(\partial S/\partial Y_l)_{P,\rho}$  determines whether the lepton gradient is stabilizing or de-stabilizing. Note that  $dY_l/dR < 0$  is quickly established by passive neutrino diffusion in a proto-neutron star. Evaluation of the derivative is greatly simplified when  $Y_\nu \ll Y_e$ , so that one can approximate  $\partial/\partial Y_l \simeq \partial/\partial Y_e$ .

We idealize the neutrons and protons as non-relativistic Fermi gases. It will prove convenient to introduce a characteristic Fermi momentum

$$p_F \equiv \hbar(3\pi^2 n_b)^{1/3} = 330 \left(\frac{n_b}{n_{\text{sat}}}\right)^{1/3} \text{ MeV}/c. \quad (\text{A13})$$

Then the Fermi energies of the neutrons and protons can be written as

$$\epsilon_{p,n} \approx \frac{\hbar^2}{2m_n} (3\pi^2 n_{p,n})^{2/3} = Y_{p,n}^{2/3} \frac{p_F^2}{2m_n}. \quad (\text{A14})$$

Here  $\hbar$  is Planck's constant. The neutrons are in fact just becoming degenerate at  $k_B T \approx 40$  MeV, which is the peak temperature generated immediately after the collapse (Pons et al. 1999); it is the associated rise in pressure that halts the collapse. The protons are less dense, and so they are only marginally degenerate. Their contribution to the entropy is smaller but significant. The analysis is simplified by treating the protons as an almost degenerate gas, but it should be kept in mind that this approximation is only marginally valid.

The electrons and electron neutrinos are, by contrast, highly relativistic (cf. equation [A13]). Their Fermi energies are

$$\epsilon_e \approx \hbar c (3\pi^2 n_e)^{1/3} = Y_e^{1/3} p_{Fc}. \quad (\text{A15})$$

and

$$\epsilon_{\nu_e} \approx \hbar c (6\pi^2 n_{\nu_e})^{1/3} = (2Y_{\nu_e})^{1/3} p_{Fc}. \quad (\text{A16})$$

Notice that

$$\frac{\epsilon_{\nu_e}}{\epsilon_e} = \left( \frac{2Y_{\nu_e}}{Y_e} \right)^{1/3} \quad (\text{A17})$$

is not necessarily small when  $Y_{\nu_e} \ll Y_e$ . We will *not* neglect terms of order  $\epsilon_{\nu_e}/\epsilon_e$  even while dropping terms of order  $Y_{\nu_e}/Y_e$ .

At finite temperature, the chemical potentials are

$$\mu_{p,n} \approx \epsilon_{p,n} \left[ 1 - \frac{\pi^2}{12} \left( \frac{k_B T}{\epsilon_{p,n}} \right)^2 \right], \quad (\text{A18})$$

and

$$\mu_{e,\nu} \approx \epsilon_{e,\nu} \left[ 1 - \frac{\pi^2}{3} \left( \frac{k_B T}{\epsilon_{e,\nu}} \right)^2 \right], \quad (\text{A19})$$

and the entropies (per baryon) are

$$\frac{S_{p,n}}{k_B} = \frac{\pi^2}{2} Y_{p,n} \left( \frac{k_B T}{\epsilon_{p,n}} \right) \quad (\text{A20})$$

and

$$\frac{S_{e,\nu}}{k_B} = \pi^2 Y_{e,\nu} \left( \frac{k_B T}{\epsilon_{e,\nu}} \right). \quad (\text{A21})$$

The pressures can be approximated as

$$P_{p,n} = \frac{2}{5} n_{p,n} \epsilon_{p,n} + \frac{1}{3} n_b S_{p,n} T \quad (\text{A22})$$

and

$$P_{e,\nu} = \frac{1}{4} n_{e,\nu} \epsilon_{e,\nu} + \frac{1}{6} n_b S_{e,\nu} T. \quad (\text{A23})$$

The key thermodynamic derivative can be expanded as

$$\left(\frac{\partial S}{\partial Y_l}\right)_{P,\rho} \simeq \left(\frac{\partial S}{\partial Y_e}\right)_{P,\rho} = \left(\frac{\partial S}{\partial Y_e}\right)_{\rho,T} + \left(\frac{\partial S}{\partial T}\right)_{\rho,Y_e} \left(\frac{\partial T}{\partial Y_e}\right)_{P,\rho}. \quad (\text{A24})$$

To evaluate this expression, we need

$$\left(\frac{\partial S}{\partial T}\right)_{\rho,Y_e} = \frac{S}{T}. \quad (\text{A25})$$

and

$$\left(\frac{\partial T}{\partial Y_e}\right)_{P,\rho} = -\frac{(\partial P/\partial Y_e)_{\rho,T}}{(\partial P/\partial T)_{\rho,Y_e}}. \quad (\text{A26})$$

The derivative  $(\partial P/\partial Y_e)_{T,\rho}$  is dominated by the (zero-temperature) degeneracy pressure

$$P_0 \equiv \frac{2}{5}n_n\epsilon_n + \frac{2}{5}n_p\epsilon_p + \frac{1}{4}n_e\epsilon_e + \frac{1}{4}n_{\nu_e}\epsilon_{\nu_e}, \quad (\text{A27})$$

so that

$$\left(\frac{\partial P_0}{\partial Y_e}\right)_{\rho} = \frac{1}{3}n_b(2\epsilon_p - 2\epsilon_n + \epsilon_e) + \frac{1}{3}n_b\epsilon_{\nu_e} \left(\frac{\partial Y_{\nu_e}}{\partial Y_e}\right)_{\rho} \quad (\text{A28})$$

Neglecting the last term on the RHS for the moment, and invoking the  $\beta$ -equilibrium condition  $\epsilon_p + \epsilon_e = \epsilon_n + \epsilon_{\nu}$ , one finds

$$\left(\frac{\partial P_0}{\partial Y_e}\right)_{\rho} = \frac{n_b}{3}(2\epsilon_{\nu} - \epsilon_e). \quad (\text{A29})$$

However, the thermal contribution to the pressure cannot be neglected,

$$\left(\frac{\partial P}{\partial Y_e}\right)_{\rho,T} = \left(\frac{\partial P_0}{\partial Y_e}\right)_{\rho} + \frac{n_b T}{3} \frac{\partial}{\partial Y_e} \left[ S_p + S_n + \frac{1}{2}(S_e + S_{\nu_e}) \right], \quad (\text{A30})$$

as it rescales the first term on the RHS of eq. (A24). Combining

$$\left(\frac{\partial P}{\partial T}\right)_{\rho,Y_e} = \frac{2}{3}n_b \left( S_p + S_n + \frac{1}{2}S_e + \frac{1}{2}S_{\nu_e} \right), \quad (\text{A31})$$

with the above equations, one finds

$$\begin{aligned} \left(\frac{\partial S}{\partial Y_e}\right)_{P,\rho} &= \frac{1}{2} \left[ \left(\frac{\partial S_n}{\partial Y_e}\right)_{\rho,T} + \left(\frac{\partial S_p}{\partial Y_e}\right)_{\rho,T} \right] \left[ \frac{S_p + S_n}{S_p + S_n + (S_e + S_{\nu_e})/2} \right] + \\ &+ \frac{3}{4} \left[ \left(\frac{\partial S_e}{\partial Y_e}\right)_{\rho,T} + \left(\frac{\partial S_{\nu_e}}{\partial Y_e}\right)_{\rho,T} \right] \left[ \frac{S_p + S_n + (S_e + S_{\nu_e})/3}{S_p + S_n + (S_e + S_{\nu_e})/2} \right] - \left[ \frac{S}{S_p + S_n + (S_e + S_{\nu_e})/2} \right] \frac{2\epsilon_{\nu_e} - \epsilon_e}{2T} \end{aligned} \quad (\text{A32})$$

Neglecting the entropy of the electrons and neutrinos compared with the nucleons, this expression simplifies to

$$\left(\frac{\partial S}{\partial Y_e}\right)_{P,\rho} = \frac{1}{2} \left(\frac{\partial S}{\partial Y_e}\right)_{\rho,T} - \frac{2\epsilon_{\nu_e} - \epsilon_e}{2T} \quad (\text{A33})$$

The variation of the entropy with lepton number is, in the same approximation,

$$\left(\frac{\partial S}{\partial Y_e}\right)_{\rho,T} = \frac{1}{3} \left(\frac{S_p}{Y_e} - \frac{S_n}{1 - Y_e}\right) = \frac{\pi^2}{3} k_B \left(\frac{k_B T}{\epsilon_e}\right) \left(\frac{m_n c^2}{\epsilon_e}\right) \left[1 - \left(\frac{Y_e}{1 - Y_e}\right)^{2/3}\right]. \quad (\text{A34})$$

A fuller evaluation of these derivatives, including the contributions from the electrons and electron neutrinos, requires knowing the quantity  $(\partial Y_{\nu_e}/\partial Y_e)_{\rho,T}$ , which can be determined directly from the condition (A4) of chemical equilibrium:  $(\partial Y_{\nu_e}/\partial Y_e)_{\rho,T} \simeq (Y_{\nu_e}/Y_e)^{2/3}$  when  $Y_{\nu_e} \ll Y_e$ . For example, substitution of this expression on the RHS of eq. (A28) shows that the derivative of the electron neutrino pressure is of order  $Y_{\nu_e}/Y_e$ , and can indeed be neglected.

The compositional gradient ( $dY_l/dR < 0$ ) tends to suppress convective instability if  $(\partial S/\partial Y_l)_{P,\rho} > 0$ , and is otherwise de-stabilizing. Both terms in eq. (A33) are positive if  $2\epsilon_{\nu} < \epsilon_e$ , that is, if  $Y_{\nu_e} < \frac{1}{16}Y_e$ . However, immediately after the collapse  $\epsilon_{\nu} \approx \epsilon_e$ , and so the composition gradient is potentially de-stabilizing. The sign of  $(\partial S/\partial Y_l)_{P,\rho}$  reverses at a critical temperature

$$kT_{\star} \equiv \frac{\epsilon_e}{\pi} \left[\frac{3(2\epsilon_{\nu} - \epsilon_e)}{m_n c^2}\right]^{1/2} \left[1 - \left(\frac{Y_e}{1 - Y_e}\right)^{2/3}\right]^{-1/2}, \quad (\text{A35})$$

which we evaluate in the main text.

This expression qualitatively reproduces the domain of convective instability in the  $S - Y_l$  plane, as plotted in Figure 1 of Lattimer & Mazuerk (1981). Those authors find that low  $Y_l$  and high  $T$  tend to suppress compositionally-driven convection. They also find that convective instability remains possible at very low entropies and lepton fractions, where heavy nuclei can form. However, that instability is restricted to densities below nuclear saturation.

### A.3. Triggering Convection

When the compositional gradient is destabilizing, convection will ensue. However, when it is stabilizing, convection may still occur if the entropy gradient is negative. Convection

occurs if

$$\frac{dS_0}{dR} < \left( \frac{\partial S}{\partial Y_l} \right)_{P,\rho} \frac{dY_{l,0}}{dR}. \quad (\text{A36})$$

The gradient of  $Y_l$  is generally negative, and we have already evaluated the thermodynamic derivative  $(\partial S/\partial Y_l)_{P,\rho}$ . It remains to re-express the entropy gradient in terms of a convective temperature gradient. Approximating

$$S \simeq S_n + S_p = \frac{p_F m_n k_B^2 T}{3 \hbar^3 n_b} \left[ Y_e^{1/3} + (1 - Y_e)^{1/3} \right], \quad (\text{A37})$$

(recall  $p_F = \hbar (3\pi^2 n_b)^{1/3}$ ), the left hand side of eqn. (A36) yields

$$\frac{d \ln S}{d \ln R} = \frac{d \ln T}{d \ln R} - \frac{2}{3} \frac{d \ln \rho}{d \ln R} + \frac{Y_e^{1/3} [(1 - Y_e)^{2/3} - Y_e^{2/3}]}{(1 - Y_e)^{2/3} [3(1 - Y_e)^{1/3} + Y_e^{1/3}]} \frac{d \ln Y_e}{d \ln R}. \quad (\text{A38})$$

We evaluate the first factor on the left hand side of eqn. (A36) at low temperatures. This allows us to neglect the first term in eq. [A33], yielding

$$\frac{Y_e}{S} \left( \frac{\partial S}{\partial Y_e} \right)_{P,\rho} \simeq \frac{3Y_e^{4/3}}{Y_e^{1/3} + (1 - Y_e)^{1/3}} \frac{\hbar^3 c n_b}{m_n (k_B T)^2} \left( \frac{2\mu_{\nu_e} - \mu_e}{2\mu_e} \right). \quad (\text{A39})$$

Using eqs. (A38) and (A39) in (A36) leads to expression (8) for the convective temperature derivative  $(d \ln T / d \ln R)_{\text{conv}}$ . In §2.1, we calculate the radiative temperature gradient associated with passive neutrino transport, and infer the critical radiative flux that drives convection.

#### A.4. The Brunt-Väisälä frequency

The electron fraction decreases outward through the degenerate core of a cold neutron star. That this compositional gradient tends to stabilize against convection was noted by Lattimer & Mazurek (1981) and demonstrated in detail by Reisenegger & Goldreich (1992) (in the approximation where the neutrons and protons are normal Fermi fluids). Here we reproduce the result of Reisenegger & Goldreich (1992).

The equation of motion for our fluid element is

$$\rho \frac{d^2 \xi}{dt^2} = F_B. \quad (\text{A40})$$

This leads to the definition of the Brunt-Väisälä frequency  $N$ ,

$$N^2 \equiv \frac{g}{\rho} \left[ \left( \frac{d\rho}{dr} \right)_{S,Y_l} - \frac{d\rho_0}{dr} \right] = -\frac{g}{\rho} \left( \frac{\partial \rho}{\partial S} \right)_{P,Y} \left[ \frac{dS_0}{dr} - \left( \frac{\partial S}{\partial Y_l} \right)_{P,\rho} \frac{dY_0}{dr} \right]. \quad (\text{A41})$$

We use the latter form in order to check our expressions for the partial derivatives by comparing to the result of Reisenegger & Goldreich (1992), who evaluate the Brunt in a cold neutron star. The star is assumed contain no neutrinos ( $Y_{\nu_e} = \epsilon_{\nu} = 0$ ), to be in chemical equilibrium ( $\epsilon_n \approx \epsilon_e$ ), and to have zero temperature and entropy. Under those conditions the Brunt reduces to

$$N^2 = \frac{g}{\rho_0} \left( \frac{\partial \rho}{\partial S} \right)_{P, Y_e} \left( \frac{\partial S}{\partial Y_e} \right)_{P, \rho} \frac{dY_e}{dr}. \quad (\text{A42})$$

From the definition  $Y_e = n_e/n_b$  we have

$$\frac{dY_e}{dr} = \frac{1}{n_b} \frac{dn_e}{dr} - \frac{Y_e}{n_b} \frac{dn_b}{dr}. \quad (\text{A43})$$

From the equilibrium condition we find

$$\alpha n_n^2 = n_e, \quad (\text{A44})$$

where  $\alpha \equiv (\hbar/2mc)^3 3\pi^2$  is a numerical constant. From charge neutrality  $n_e = n_p$ , conservation of baryon number gives  $n_n + n_e = n_b$ . Taking the derivative of this expression with respect to radius, and solving for the electron density gradient, we find

$$\frac{dn_e}{dr} = 2Y_e \frac{dn_b}{dr} + O(Y_e)^2. \quad (\text{A45})$$

Combining these results in

$$\frac{dY_e}{dr} = \frac{Y_e}{\rho_0} \frac{d\rho_0}{dr}. \quad (\text{A46})$$

Finally we evaluate the variation of density with entropy at fixed pressure and composition. We have

$$\left( \frac{\partial S}{\partial \rho} \right)_{P, Y_i} = \left( \frac{\partial S}{\partial \rho} \right)_{T, Y_i} - \left( \frac{\partial S}{\partial T} \right)_{\rho, Y_i} \frac{(\partial P / \partial \rho)_{T, Y_i}}{(\partial P / \partial T)_{\rho, Y_i}}. \quad (\text{A47})$$

From equations (A20-A23) we find

$$\left( \frac{\partial S}{\partial \rho} \right)_{T, Y_e} = -\frac{2S}{3\rho}, \quad (\text{A48})$$

$$\left( \frac{\partial P}{\partial \rho} \right)_{T, Y_e} = \frac{5P}{3\rho}, \quad (\text{A49})$$

and

$$\left( \frac{\partial P}{\partial T} \right)_{\rho, Y_e} = -\frac{2}{3} n_b S, \quad (\text{A50})$$

where we neglect the leptonic contribution to the entropy. Combining these with eqn. (A25) we find

$$\left(\frac{\partial S}{\partial \rho}\right)_{P, Y_e} = -\left(\frac{2S}{3\rho}\right) - \left(\frac{5S}{2\rho}\right) \frac{P}{n_b S T}. \quad (\text{A51})$$

The second term on the right-hand side of this equation is much larger than the first:  $P/n_b S T \approx (4/5\pi^2)(\epsilon_n/k_b T)^2 \gg 1$ . To lowest order in  $k_b T/\epsilon_b$

$$\left(\frac{\partial \rho}{\partial S}\right)_{P, Y_e} = -\frac{\pi^2}{2} \left(\frac{k_b T}{\epsilon_n}\right)^2 \frac{\rho}{S} = -\frac{T}{\epsilon_n} \frac{\rho}{Y_n}. \quad (\text{A52})$$

Using equations (A33), (A46), and (A52)

$$N^2 = \frac{g}{\rho_0} \left(-\frac{T}{\epsilon_n} \frac{\rho_0}{Y_n} \frac{\epsilon_n}{2T}\right) \frac{Y_e}{\rho_0} \frac{d\rho_0}{dr} = \frac{Y_e}{2Y_n} \frac{g}{H}, \quad (\text{A53})$$

where  $H \equiv -\rho/(d\rho_0/dr)$ . This is the expression found by Reisenegger & Goldreich (1992).

## REFERENCES

- Bethe, H.A., & Wilson, J.R. 1985, ApJ, 295, 14
- Bruenn, S.W., & Mezzacappa, A. 1994, ApJ, 433 L45
- Burrows, A. 1987, ApJ, 318, L57
- Burrows, A., Hayes, J., & Fryxell, B.A. 1995, ApJ, 450, 830
- Burrows, A., & Lattimer, J.M. 1986, ApJ, 307, 178
- Delfosse, X., Forveille, T, Perrier, C. Mayor, M. 1998, A&A, 331, 581
- Dorch, S.B.F. & Nordlund, Å. 2000, A&A, in press ([astro-ph/0006358](#))
- Duncan, R.C., & Thompson, C. 1992, ApJ, 392, L9
- Durney, B.R., de Young, D.S., & Roxburgh, I.W. 1993, Solar Phys., 145, 207
- Fryer, C., Colgate, S.A., & Pinto P.A. 1999, ApJ, 511, 885
- Geppert, U., Page, D. & Zannias, T. 1999, A&A, 345, 847
- Goldreich, P., & Reisenegger, A. 1992, ApJ, 395, 250
- Goldreich, P., Murray, N., Willette G., & Kumar, P. 1991, ApJ, 370, 752
- Iwamoto, N. 1981, Ph.D. Thesis, University of Illinois, Urbana
- Janka, H.T. & Müller, E. 1996, A&A, 306, 167
- Keil, W., Janka, H.-T., Müller, E. 1996, ApJ, 473, 111 (KJM)
- Kluzniak, W. & Ruderman, M. 1998, ApJ, 508, L113
- Kouveliotou, C., Dieters, S., Strohmayer, T., van Paradijs, J., Fishman, G., Meegan, C.A., Hurley, K., Kommers, J., Smith, I., Frail, D., Murakami, T. 1998, Nature, 393, 235
- Kouveliotou, C., Strohmayer, T., Hurley, K., van Paradijs, J., Finger, M.H., Dieters, S., Woods, P., Thompson, C., & Duncan R.C. 1999, ApJ, 510, 115
- Küker, M., & Rüdiger, G. 1999, A&A, 346, 922
- Kulkarni, S.R. 1992, Phil. Trans. R. Soc. Lond. A, 341, 77
- Lattimer, J.M., & Mazurek, T.J. 1981, ApJ, 246, 955

- Lyne, A.G., & Manchester, R.N. 1989, M.N.R.A.S., 234, 477
- Mayle, R.W., & Wilson J.R. 1989, preprint
- Meneguzzi, M., & Pouquet, A. 1989, J. Fluid Mech., 205, 297
- Mezzacappa, A., Calder, A.C., Bruenn, S.W., Blondin, J.M., Guidry, M.W., Strayer, M.R., & Umar, A.S. 1998, ApJ, 495, 911
- Murray, N. 1992, Sol. Phys., 138, 419
- Parker, E. 1979, *Cosmical Magnetic Fields* (Oxford Univ. Press)
- Pethick, C.J., in *Structure and Evolution of Neutron Stars*, ed. D. Pines, R. Tanigaki, & S. Tsuruta (Redwood City: Addison-Wesley), 115
- Pons, J.A., Reddy, D., Prakash, M., Lattimer, J.M., & Miralles, J.A. 1999, ApJ, 513, 780
- Reddy, S., Prakash, M., & Lattimer J.M. 1998, Phys. Rev. D, 58, 013009
- Reisenegger, A., & Goldreich, P. 1992, ApJ, 395, 240
- Ruzmaikin, A.A. & Sokoloff, D.D. 1981, Soviet Astron. Lett., 7(6), 388
- Ruzmaikin, A.A., Vainshtein, S.I. 1978, Ap & SS, 57, 195
- Stenflo, J.O. 1989, A&ARv, 1, 3
- Thelen, J.-C., & Cattaneo, F. 2000, MNRAS, 315, L13
- Thompson, C. 2000, ApJ, 534, 915 (T00)
- Thompson, C., & Duncan, R.C. 1993, ApJ, 408, 194 (TD93)
- Thompson, C., & Duncan, R.C. 1996, ApJ, 473, 322
- Tobias, S.M., Brummell, N.H., Clune, T.L., Toomre, J. 1998, ApJ, 502, L177
- Wilson, J.R., & Mayle, R.W. 1985, Phys. Rep. 163, 63
- Woosley, S.E., Weaver, T.A. 1995, ApJS, 101, 181

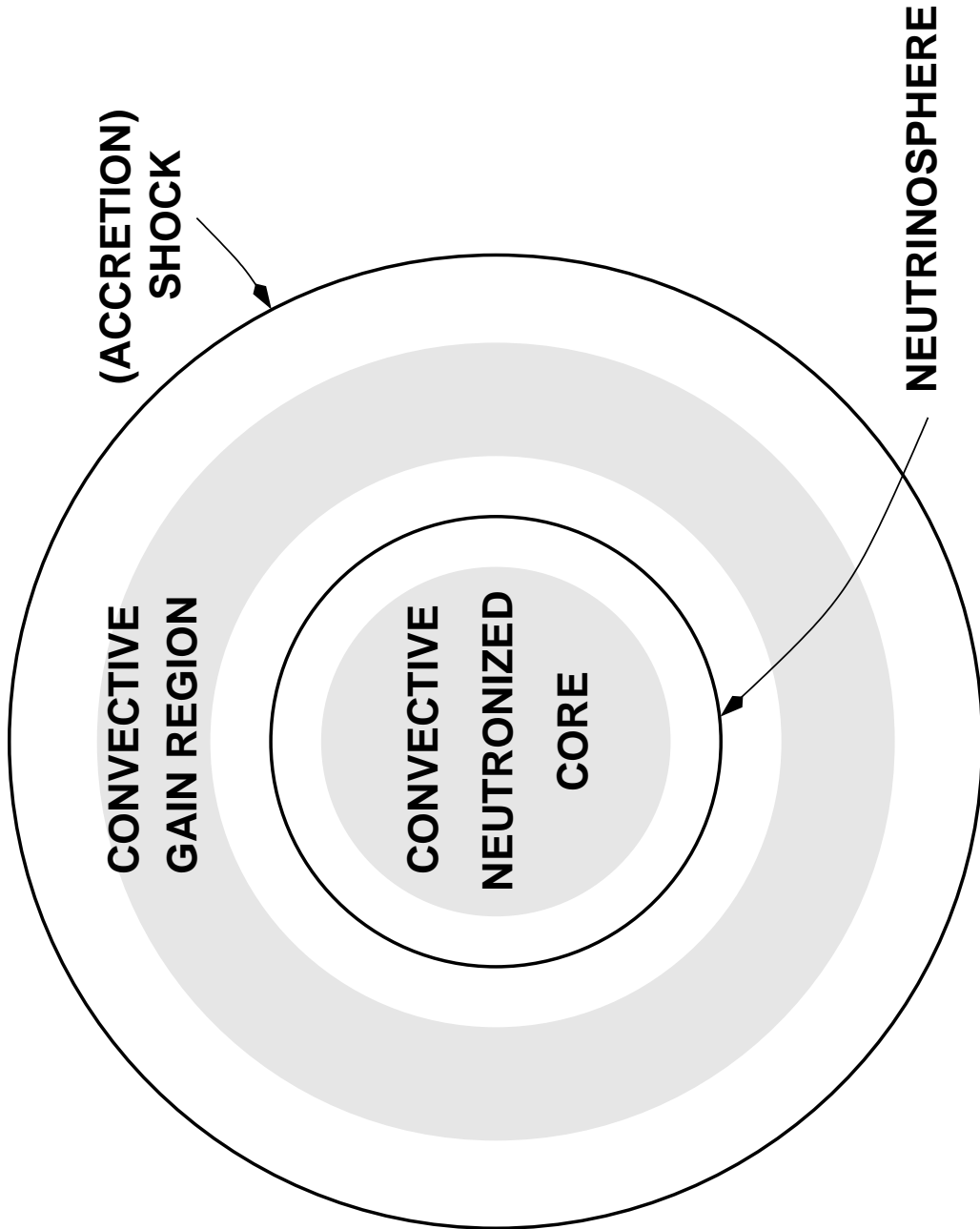


Fig. 1.— The collapsed core of a massive star develops a violent convective instability in two distinct regions: within the central, neutronized core which is optically thick to neutrinos; and outside the neutrino photosphere, within a spherical shell where heating by the charged-current absorption of  $\nu_e$  and  $\bar{\nu}_e$  on free  $n, p$  is faster than cooling by captures of electron-positron pairs. The region straddling the  $\nu$ -sphere is, typically, stable to convection.

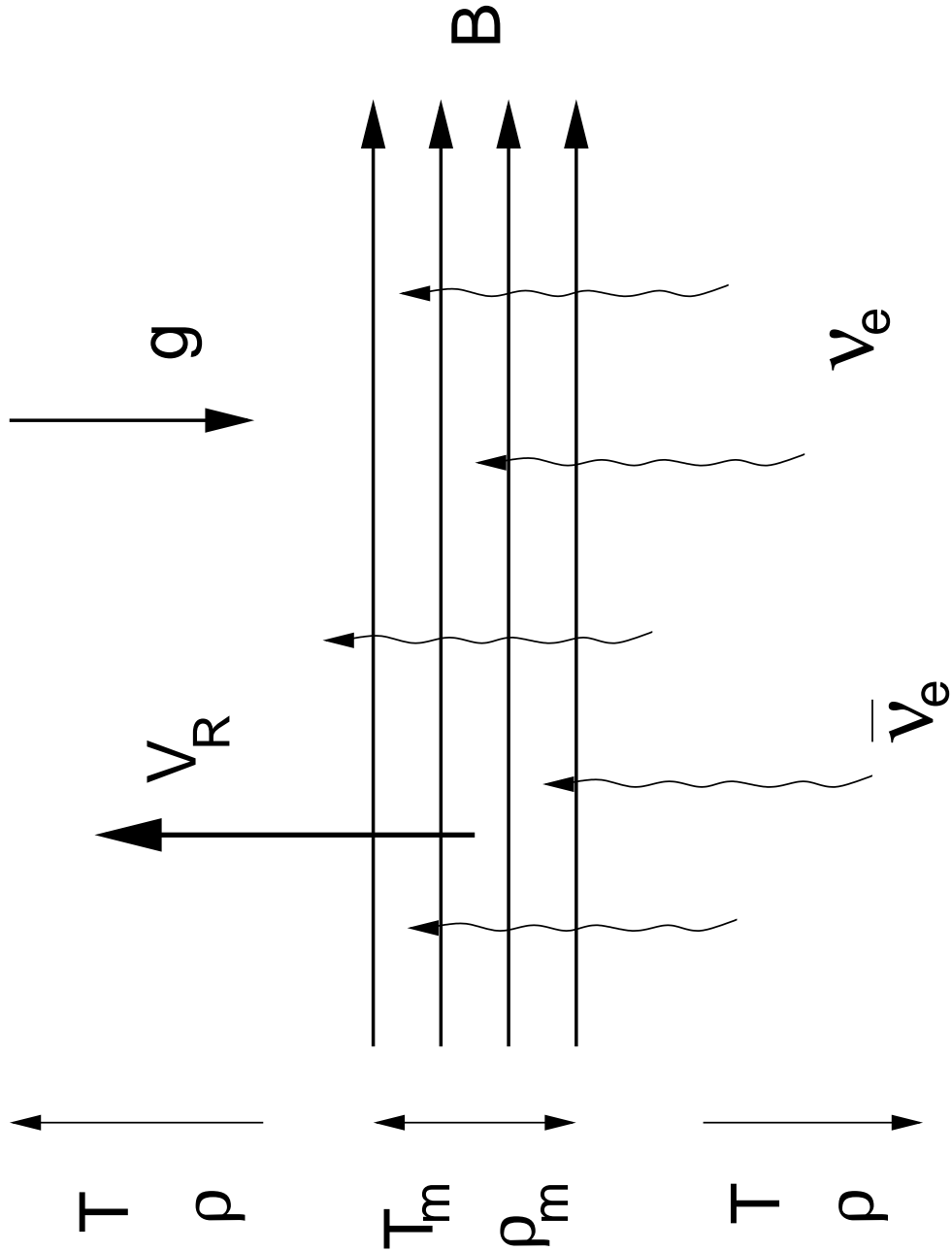


Fig. 2.— A horizontal bundle of magnetic flux has a lower temperature than its surroundings,  $T_M < T$ , at constant density and pressure. Electron-type neutrinos, originating outside the bundle, raise its temperature and allow it to move upward through a stabilizing composition (or entropy) gradient.

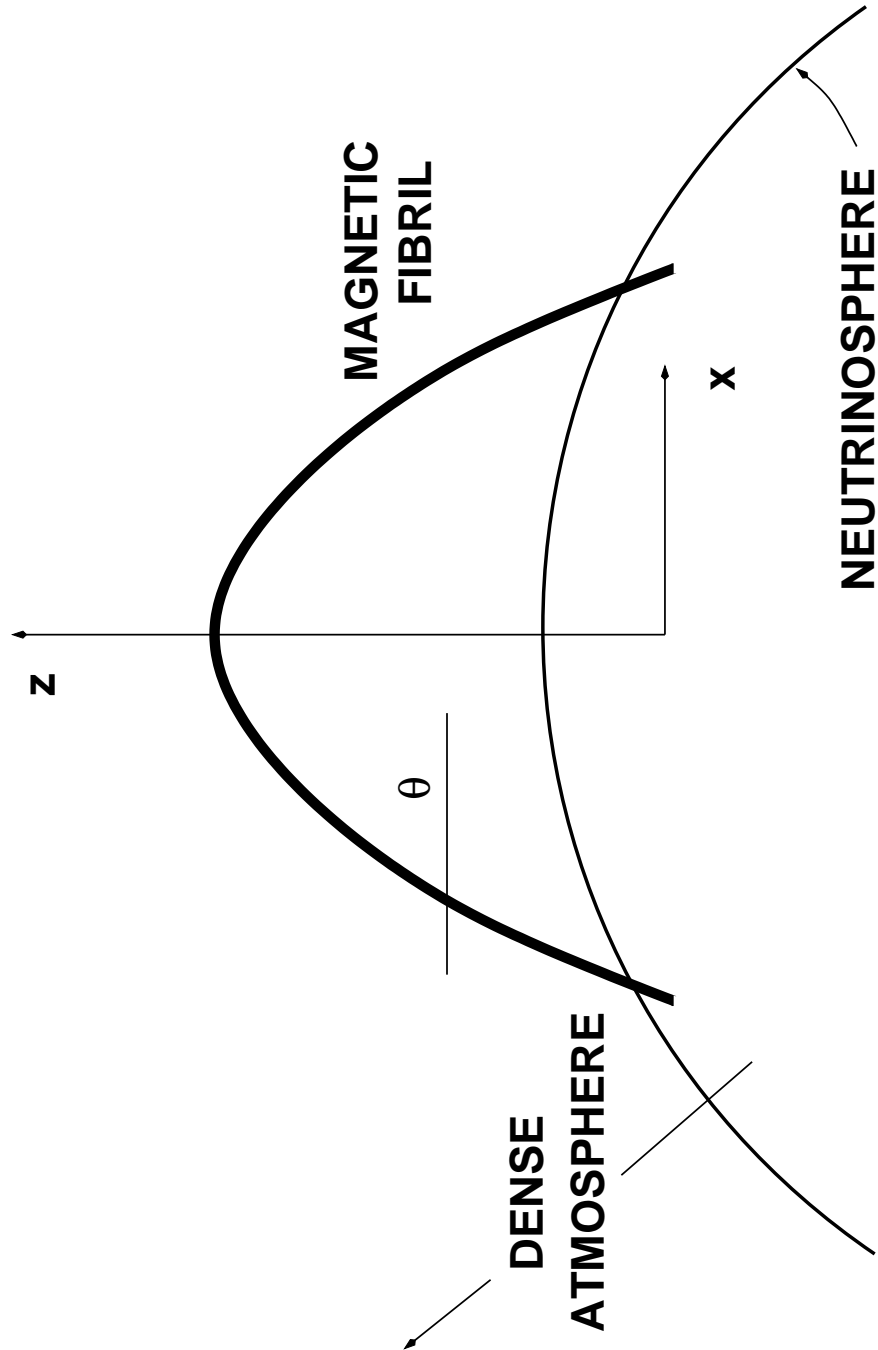


Fig. 3.— A narrow bundle of magnetic flux reaches an equilibrium configuration which is a competition between buoyancy and tension forces. When the separation between the magnetic footpoints exceeds a critical value, the equilibrium bundle reaches to infinite height (radius).